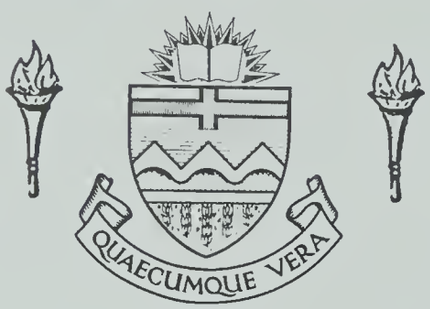

THE UNIVERSITY OF ALBERTA

DYNAMIC RESPONSE OF THIN ELASTIC ARCHES

BY

© ALEXANDER SEMENIUK

A THESIS

SUBMITTED TO THE FACULTY OF GRADUATE STUDIES

IN PARTIAL FULFILMENT OF THE REQUIREMENTS FOR THE DEGREE

OF DOCTOR OF PHILOSOPHY

DEPARTMENT OF MECHANICAL ENGINEERING

EDMONTON, ALBERTA

SPRING, 1971

UNIVERSITY OF ALBERTA

FACULTY OF GRADUATE STUDIES

The undersigned certify that they have read, and recommend to the Faculty of Graduate Studies for acceptance, a thesis entitled "DYNAMIC RESPONSE OF THIN ELASTIC ARCHES" submitted by ALEXANDER SEMENIUK in partial fulfilment of the requirements for the degree of Doctor of Philosophy.

Abstract

A theory is presented which can be used to investigate the dynamic response of arches subjected to cyclic support movement. The theory assumes that the arch is circular having a constant mass per unit arch length, the cross-section is constant, damping is small and the center line of the arch is inextensible. The effects of rotatory inertia and shear deflections are assumed small, compared with the effects of flexure, and are neglected. Only deflections in the plane of the initial curvature of the arch are considered. A closed form solution is obtained for free vibrations and an eight-term series in terms of the free modes of vibration is used to evaluate the steady state solution for forcing frequencies up to the fourth free flexural mode. Experimental evaluation of the theory is presented on the basis of radial displacements for arches having pinned-end boundary conditions.

Results are presented for arches having radius to thickness ratio from 121.2 to 179.4 and half-opening angles of 97.2 to 119.2 degrees for forcing frequencies up to the fourth flexural mode of free vibration. For some arches tested, out-of-plane displacements were noted to occur at frequencies having values approximately sixteen times the value of the frequency for the first free flexural mode. A discussion of the parameters that influence the agreement between the theoretical and the experimental results is included in the presentation of experimental data.

Acknowledgment

The author wishes to thank Dr. D.G. Bellow for the guidance and supervision received during the course of this research. He also appreciates the interest shown and the numerous suggestions and comments made by Dr. J.S. Kennedy regarding this investigation. The financial support received from the National Research Council and the University of Alberta for this research is gratefully acknowledged. Thanks are also extended to P.A. Bradbury, A.G. Haliburton, R.E. Beliveau and A. Smart from the Mechanical Engineering Shop for the care taken in building the experimental apparatus; F. Christopher for ensuring the correct operation of the electrical equipment; Miss H. Wozniuk for typing this thesis and to H. Schroeder for taking the photographs.

Table of Contents

Table of Contents (continued)

List of Tables

List of Figures

List of Figures (continued)

Notation

All symbols are defined when used, however, a summary of the more commonly used symbols are listed below.

C_{ij}	constant
$D_j(t)$	time dependent function for steady state solution
D_j'	constant in the steady state solution
E	Young's Modulus
G	amplitude of support movement
g(t)	function describing support movement
H	arch thickness
I	second moment of area of the cross-section about the centroidal axis
k	radius of gyration
m	mass per unit length of arch
$P_R(\phi,t)$	external radial load per unit arch length
$P_T(\phi,t)$	external tangential load per unit arch length
R	radius of curvature
$\mathcal{R}$	Rayleigh quotient
r_n	roots to an auxiliary equation
t	time coordinate
$u(\phi,t)$	radial displacement
$u_p(\phi,t)$	radial steady state displacement

$U_n(\phi)$ n-th radial mode shape

$U_A(\phi)$ absolute steady state radial displacement

U_A/G radial magnification ratio

$v(\phi,t)$ tangential displacement

$v_p(\phi,t)$ tangential steady state displacement

$V_n(\phi)$ n-th tangential mode shape

$V_A(\phi)$ absolute steady state tangential displacement

V_A/G tangential magnification ratio

$w(\phi,t)$ represents either $v(\phi,t)$ or $u(\phi,t)$

$W_n(\phi)$ represents either $V_n(\phi)$ or $U_n(\phi)$

$( )^I, ( )^{II}$, etc. means $\frac{d( )}{d\phi}$, $\frac{d^2( )}{d\phi^2}$, etc.

$(\dot{\ }), (\ddot{\ })$ means $\frac{d( )}{dt}$, $\frac{d^2( )}{dt^2}$

Greek Symbols

α one-half the arch opening angle

ϕ angular coordinate

λ_n n-th dimensionless frequency ($\lambda_n = \frac{\omega_n}{R^2}\sqrt{\frac{EI}{m}}$)

ω_n n-th natural frequency

Ω frequency of support movement

κ curvature (1/R)

$\eta(t)$ time dependent function

Object and Scope

The purpose of this study was to:

(a) develop and present a theoretical method for evaluating the dynamic response of circular arches subjected to cyclic support movement, and

(b) experimentally evaluate the theory.

To simplify the analysis, a circular arch with a constant cross-section and constant mass per unit length was chosen. Only flexural deflections in the plane of the initial curvature of the arch were studied. In the theoretical analysis, a closed form solution for the governing differential equations was obtained for arches having various types of boundary conditions. The experimental investigation was restricted to arches having pinned ends.

Chapter I

Introduction and Literature Review

1.1 Introduction

This thesis consists of a review, in Chapter I, of pertinent previous investigations dealing with deep arches i.e. opening angle greater than 80 degrees, that have been reported in the literature. On the basis of this review, the theoretical analysis is summarized in Chapter II and, where necessary, expanded to meet the objectives of this investigation. Chapter III contains a discussion of the experimental technique and a description of the experimental apparatus used. A comparison between theoretical and experimental results for four arches, having radius to thickness ratios in the range $121.2 \leq \frac{R}{H} \leq 179.4$ and one-half opening angles in range $97.2 \leq \alpha \leq 119.2$ degrees, for pinned-end boundary conditions is also presented in Chapter III. Chapter IV contains a summary of the more important observations arising from the investigations and a list of some associated problems suggested for further study.

The coordinate system and components of displacement of a point on the middle surface of the arch are shown in Fig. 1.1-1.

The notation used is:

b arch width

E Young's Modulus

H arch thickness

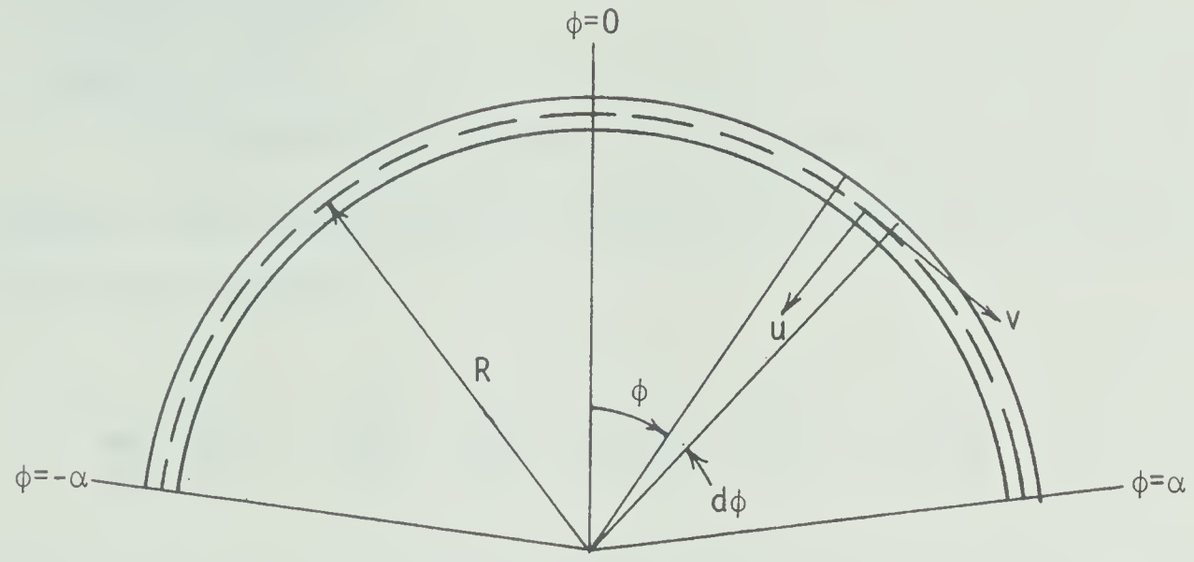

FIG. 1.1-1 COORDINATE SYSTEM AND COMPENENTS OF DISPLACEMENT

I	second moment of area of the cross-section about the centroidal axis
m	mass per unit length of arch
R	radius of curvature
t	time coordinate
$u(\phi,t)$	radial displacement measured from the undeformed shape of the arch
$v(\phi,t)$	tangential displacement measured from the undeformed shape of the arch
α	one-half the arch opening angle
ϕ	angular coordinate

1.2 Literature Review

Lamb (1, 1888)

Considering an element of an arch and using a combination of potential energy techniques and calculus of variations, Lamb obtained the following equation:

$$\frac{EI}{mR^4}\left(\frac{\partial^6 v}{\partial\phi^6} + 2\frac{\partial^4 v}{\partial\phi^4} + \frac{\partial^2 v}{\partial\phi^2}\right) + \left(\frac{\partial^4 v}{\partial\phi^2\partial t^2} - \frac{\partial^2 v}{\partial t^2}\right) = \frac{1}{m}\left(\frac{\partial P_R}{\partial\phi} - P_T\right) \qquad 1.2\text{-}1$$

where $P_T(\phi,t)$ and $P_R(\phi,t)$ are external loads acting in the tangential and radial directions respectively. In deriving eq. 1.2-1 Lamb assumed the mid-surface of the arch to be inextensible which relates u and v through the equation

$$u = \frac{\partial v}{\partial\phi} \quad . \qquad 1.2\text{-}2$$

For the case of free vibration ($P_R = P_T \equiv 0$), Lamb assumed the tangential displacement as

$$v = \sum_{n=1}^{\infty} V_n(\phi)\, e^{i\,\omega_n t} \quad . \qquad 1.2\text{-}3$$

Substituting eq. 1.2-3 into 1.2-1, yields

$$V_n^{VI} + 2V_n^{IV} + V_n^{II}(1-\lambda_n^2) + \lambda_n^2 V_n = 0 \qquad 1.2\text{-}4$$

where

$$\lambda_n^2 = \omega_n^2 \frac{mR^4}{EI} \qquad 1.2\text{-}5$$

and the notation $(\ )^{I}$, $(\ )^{II}$, etc. denotes differentiation with respect to the angular coordinate ϕ. When the assumed solution

$$V_n = \sum_{j=1}^{6} C_{nj} e^{r_{nj}\phi}$$

was substituted into eq. 1.2-4, Lamb obtained

$$r_n^6 + 2r_n^4 + r_n^2 (1-\lambda_n^2) + \lambda_n^2 = 0 . \qquad 1.2\text{-}6$$

Lamb did not obtain a solution to eq. 1.2-6 for the general case, but he did obtain some results for a shallow arch by noting that one root of the cubic in r_n^2 is nearly equal to unity and approximating the remaining roots by $r_n^2 + 1 = \pm \lambda$. With this approximation, the mode shapes and the natural frequencies for the lower modes were obtained.

By neglecting the inertia terms and external loads in eq. 1.2-1 Lamb also solved for the deflection of arches under various static loads acting at the boundaries, $\phi = \pm \alpha$, of the arch.

Den Hartog (2, 1928)

By use of the Rayleigh quotient, Den Hartog calculated the lowest natural frequency of circular arches subtending any angle up to 360 degrees, for pinned and clamped ends. For the tangential displacement he assumed a function

$$v = \frac{A\alpha}{\pi} \left(\cos \frac{\pi\phi}{\alpha} + 1\right) \sin \omega t$$

and by satisfying inextensibility, the radial displacement was

$$u = A \sin \frac{\pi\phi}{\alpha} \sin \omega t$$

for pinned-end boundary conditions. Using the above displacements, the maximum strain and kinetic energies were equated and the natural frequency ω was obtained. Den Hartog stated that for $30° < \alpha < 135°$, displacements of the form

$$u = 2A \left[\frac{\phi}{2\alpha} - \frac{40}{7} \left(\frac{\phi}{2\alpha}\right)^3 + \frac{48}{7} \left(\frac{\phi}{2\alpha}\right)^5\right] \sin \omega t$$

and

$$v = A\alpha \left[\frac{3}{28} - \left(\frac{\phi}{2\alpha}\right)^2 + \frac{20}{7} \left(\frac{\phi}{2\alpha}\right)^4 - \frac{16}{7} \left(\frac{\phi}{2\alpha}\right)^6\right] \sin \omega t$$

yield smaller and therefore better results for ω. Upon checking the frequency equation Den Hartog obtained by using the polynomial displacements, an error was noted, and in fact the polynomial solution yields higher and therefore poorer values for the natural frequency than does the assumed sinusoidal displacement for all values of α. The equation Den Hartog obtained was

$$\lambda^2 = \frac{1}{\alpha^4} \frac{\alpha^4 - 78.5\alpha^2 + 1585}{1 + 0.094\ \alpha^2}$$

whereas the equation should have read

$$\lambda^2 = \frac{1}{\alpha^4} \frac{\alpha^4 - 79.20\alpha^2 + 1584}{1 + 0.07769\,\alpha^2} \quad .$$

Using an analysis similar to that above, Den Hartog also evaluated natural frequencies for fixed-end boundary conditions. Den Hartog investigated extensional arches, noting that for certain R/k (k = radius of gyration of the cross-section) and α values, the extensional mode had a lower natural frequency than the inextensional mode.

Love (3, 1944)

Love used the classical approach to obtain the governing differential equation for a thin arch by applying conditions of dynamic equilibrium to an element cut from the arch as shown in Fig. 1.2-1.

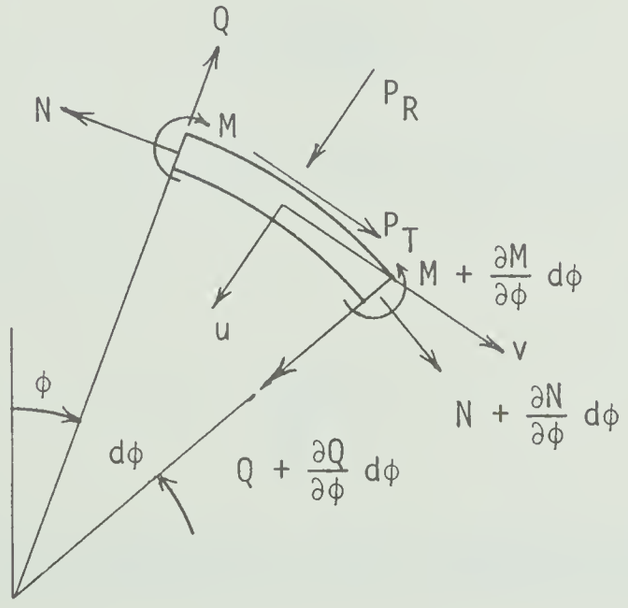

FIG. 1.2-1 ELEMENT CUT FROM ARCH

Since Love investigated free vibration, the external loads P_R and P_T are zero for this case. The three equations obtained were:

$$\frac{\partial Q}{\partial \phi} + N - mR \frac{\partial^2 u}{\partial t^2} = 0 \qquad 1.2\text{-}7$$

$$\frac{\partial N}{\partial \phi} - Q - mR \frac{\partial^2 v}{\partial t^2} = 0 \qquad 1.2\text{-}8$$

and

$$\frac{1}{R} \frac{\partial M}{\partial \phi} = Q \ , \qquad 1.2\text{-}9$$

where rotatory inertia and shear deflection effects were assumed to be negligible compared with the effects of flexure. The bending moment M and normal force N, expressed in terms of the displacements, are

$$M = - \frac{EI}{R^2} \left(\frac{\partial^2 u}{\partial \phi^2} + u \right) \qquad 1.2\text{-}10$$

and

$$N = \frac{EA}{R} \left(\frac{\partial v}{\partial \phi} - u \right) \ . \qquad 1.2\text{-}11$$

For inextensibility of the center line, the tangential and radial displacements are related by

$$\frac{\partial v}{\partial \phi} = u \ . \qquad 1.2\text{-}12$$

Combining eqs. 1.2-7 through to 1.2-12, Love obtained the equation

$$\frac{EI}{mR^4}\left(\frac{\partial^6 w}{\partial\phi^6} + 2\frac{\partial^4 w}{\partial\phi^4} + \frac{\partial^2 w}{\partial\phi^2}\right) + \frac{\partial^4 w}{\partial\phi^2\partial t^2} - \frac{\partial^2 w}{\partial t^2} = 0 \qquad 1.2\text{-}13$$

where w represents either the tangential displacement v or the radial displacement u. The solution to eq. 1.2-13 was of the form

$$w(\phi,t) = \sum_{n=1}^{\infty} W_n(\phi)\cos(\omega_n t + \theta) \qquad 1.2\text{-}14$$

which upon substituting into eq. 1.2-13, resulted in an equation, with one independent parameter ϕ, of the form

$$W_n^{VI} + 2W_n^{IV} + W_n^{II}(1-\lambda_n^2) + \lambda_n^2 W_n = 0 \qquad 1.2\text{-}15$$

where λ_n^2 is given by eq. 1.2-5. A comparison of eq. 1.2-15, as obtained by Love, with eq. 1.2-4, as obtained by Lamb, reveals that they are identical. A solution for $W_n(\phi)$ was

$$W_n(\phi) = \sum_{k=1}^{3}\left(A_{nk}\cos r_{nk}\phi + B_{nk}\sin r_{nk}\phi\right)$$

where r_n is obtained from

$$r_n^2(r_n^2-1)^2 - (r_n^2+1)\lambda_n^2 = 0 \qquad 1.2\text{-}16$$

which is identical to eq. 1.2-6 as obtained by Lamb. For a complete ring r_n must be an integer, and there are vibrations with r_n wavelengths

to the circumference, r_n being any integer greater than unity. The natural frequencies of vibration for a complete ring are given by

$$\omega_n^2 = \frac{EI}{mR^4} \frac{r_n^2(r_n^2-1)^2}{r_n^2+1} \quad . \qquad 1.2\text{-}17$$

Hoppe (4) is credited for obtaining eq. 1.2-17 in 1871.

Love suggests a method for obtaining values of r_n which determine the natural frequencies of vibration for complete rings, however, no values of r_n for arches with specific opening angles and boundary conditions were recorded.

Bolotin (5, 1952; 6, 1953; 25, 1956)

Using the basic equations developed by Lamb, Bolotin solved the stability problem of arches under parametric excitation at the crown ($\phi = 0$) of the arch. Lamb's equations were modified to account for the dynamic load acting at the crown. Bolotin investigated this problem experimentally obtaining good agreement between theory and experiment, however, the experimental details were not given. Another aspect of Bolotin's work (25) involved investigating the dynamic response of arches and rings subjected to pulsating pressure loads.

Morley (7, 1957)

Morley calculated the natural frequencies and normalized mode shapes for the first 20 free modes of vibration for a thin elastic arch subtending an angle of 360 degrees having free-end boundary conditions.

Morley's approach to the cut-ring problem was identical to the method used by Love to solve for the modal characteristics of a complete ring. However, since the ring was cut, the roots of eq. 1.2-16 are no longer integers but are determined by satisfying the free-end boundary conditions. In satisfying the boundary conditions, Morley solved for the eigenvalues of a matrix from which it was possible to calculate the natural frequencies. The eigenvectors associated with these eigenvalues determined the mode shapes. Results were not presented for any other boundary conditions or arch opening angles.

Archer (8, 1959)

In-plane, inextensional vibrations of an arch were studied by Archer, using the basic equations as derived by Love, with the addition of terms to represent damping effects. This equation can be represented as

$$\frac{EI}{mR^4}\left(\frac{\partial^6 v}{\partial\phi^6} + 2\frac{\partial^4 v}{\partial\phi^4} + \frac{\partial^2 v}{\partial\phi^2}\right) + \frac{\partial^4 v}{\partial\phi^2\partial t^2} - \frac{\partial^2 v}{\partial t^2} + \frac{c}{m}\left(\frac{\partial^3 v}{\partial t\partial\phi^2} - \frac{\partial v}{\partial t}\right) = 0 \qquad 1.2\text{-}18$$

where c represents the viscous damping coefficient. Archer solved eq. 1.2-18 by using a product solution of the form

$$v(\phi,t) = V(\phi)\ T(t) \qquad 1.2\text{-}19$$

which separated eq. 1.2-18 into

$$\frac{EI}{mR^4}\left(V^{VI} + 2\,V^{IV} + V^{II}\right) + \omega^2\left(V - V^{II}\right) = 0 \qquad 1.2\text{-}20$$

and

$$\frac{d^2T}{dt^2} + \frac{c}{m}\frac{dT}{dt} + \omega^2 T = 0\ . \qquad 1.2\text{-}21$$

Love's approach was used to reduce eq. 1.2-20 to eq. 1.2-17. In a similar approach to that of Morley, Archer solved for the roots of eq. 1.2-17.

Archer extended the solution of eq. 1.2-20 to find the transient response of a semi-circular arch under a small step motion of one support relative to the other. The particular problem was defined by assuming one support, say $\phi = \alpha$, was initially displaced tangentially by a small amount $R\,\Delta\psi$, where $\Delta\psi$ defines the change in slope between the deformed and undeformed state at the support. The end was now allowed to return to its natural position according to the motion

$$v(\alpha,t) = R\,\Delta\psi\, e^{-at}\ ,\ t > 0\ . \qquad 1.2\text{-}22$$

Equation 1.2-22, represents a time-dependent boundary condition. In obtaining a solution, Archer employed a method developed by Mindlin and Goodman (9) for solving problems with time dependent boundary conditions.

Eppink and Veletsos (10, 1959; 11, 1960; 12, 1960)

Eppink and Veletsos described a numerical procedure which can be used for computing the dynamic response of circular arches subjected to transient forces for both the elastic range of behavior and for the range approaching failure. The problem was analyzed approximately by replacing the continuous arch by a framework consisting of a series of rigid bars and flexible joints. Any external loads were assumed to be concentrated at the joints. The authors evaluated the natural frequencies and corresponding modes for a two-hinged and for a fixed arch of constant cross-section. In particular, the authors considered time-dependent pressure as the external load acting on the arch. This method of analysis permitted a calculation of the critical pressure load necessary to buckle the arch.

This work was extended (11) to include the behavior of arches in the inelastic range by approximating the cross-sectional area of the arch by two flanges connected by a thin rigid web. The resistance of each flange was represented by a bilinear stress-strain diagram. The authors obtained results for a uniform all-around pressure with a time-dependent variation represented by a triangle with an initial peak and for a triangular moving pressure pulse. The authors also investigated the effects of load parameters such as duration of pressure pulse, magnitude of peak pressure compared to the critical buckling pressure and the velocity of propagation of the pressure front. The effects of arch parameters, i.e. geometric and physical properties, were also investigated.

The previous method of analysis was applied to a two-hinged arch, of uniform cross-section and mass per unit length, which was subjected to a pressure uniformly distributed around the arch (12). The resulting governing equations were evaluated on a computer using a step-by-step method of integration. These results and the results from the modal method were compared showing good agreement between the two methods.

Volterra and Morell (13, 1960; 14, 1961; 15, 1961; 26, 1967)

Volterra and Morell extended the Rayleigh-Ritz method, used by Den Hartog, to find the lowest natural frequency of elastic arches having the center-line in a form of a cyloid, parabola, catenary, as well as a circle subjected to clamped-end boundary conditions (13). This investigation was extended (14) to include vibrations outside the plane of initial curvature of the arch. A correction to the results presented in this paper (14) was given in (26). For hinged boundary conditions (15) the lowest natural frequency was determined for arches vibrating either in the plane or out-of-the plane of the initial curvature. For in-plane vibrations, they obtained the natural frequency to be

$$\omega^2 = \frac{EI}{mR_0^4} F(\alpha) \qquad 1.2\text{-}23$$

where

$$F(\alpha) = \frac{R_0^4 \left[1 - \left(\frac{\pi}{\alpha}\right)^2\right]^2 \int_0^{\alpha} \frac{1}{R^3} \sin^2 \frac{\pi\phi}{\alpha} \, d\phi}{\int_0^{\alpha} \left(R\left[\sin^2 \frac{\pi\phi}{\alpha} + \left(\frac{\alpha}{\pi}\right)^2 \left(1 + \cos \frac{\pi\phi}{\alpha}\right)^2\right]\right) d\phi} \quad .$$

For a particular case of a circle, $R = R_0$, eq. 1.2-23 reduces to

$$\omega = \frac{\lambda}{R^2} \sqrt{\frac{EI}{m}}$$

which is identical to the result obtained by Den Hartog. The function $F(\alpha)$ can be evaluated for a cycloid, catenary and parabola by substituting for R the values $R = R_0 \cos \phi$, $R = R_0/\cos^2\phi$ and $R = R_0/\cos^3\phi$ respectively and performing the necessary integration. These authors presented results only for arches with maximum opening angles of up to 80 degrees.

Lang, T.E. and Reed, R.E. (16, 1962)

Lang and Reed also presented an approximate method for determining in-plane and out-of-plane natural frequencies and mode shapes for arches and complete circular rings with non-uniform stiffness and mass distribution. The ring was idealized by a series of point masses connected by massless elastic arch segments. The transfer matrix technique was used to obtain a solution. These results were compared to the closed form solution obtained by Love (3) (Hoppe (4), 1871) for the natural frequencies for a thin, constant thickness complete ring

with resulting differences of 0, 1, and 4.1 percent for the second, fourth and sixth mode respectively, for in-plane flexural vibrations. For out-of-plane vibrations the differences in the natural frequencies were 0, 0, 1.5, and 8.9 percent for the second, fourth, sixth and eight mode respectively. In all cases where differences occurred, the approximate technique gave lower values for the natural frequencies than those obtained from the closed form solution. The authors attributed the lower values to the fact that Hoppe did not take into account the effects of rotatory inertia.

Nelson (17, 1962)

A modification of the Rayleigh-Ritz technique, as used by Den Hartog (2), was made by Nelson by introducing Lagrangian multipliers to take into account the boundary conditions. For the unsymmetrical modes with pinned-end boundary conditions, the radial displacement was assumed to be

$$U = \sum_{n=2,4,}^{\infty} A_n \sin \frac{n\pi\phi}{2\alpha}$$

which was used together with the inextensibility condition given by eq. 1.2-2 to evaluate the energy function defined as

$$W - R\,\overline{T}$$

where W is the strain energy, $\overline{T}$ is the "reduced kinetic energy" and R is

the Rayleigh quotient. An extremum of the energy function was then found with respect to the A_n's and a constant B which was obtained from evaluating the tangential displacement V by using eq. 1.2-2, i.e.

$$V = \int_{-\alpha}^{\alpha} U \, d\phi + B \, .$$

Introducing the Lagrangian multiplier γ, the energy function was written as

$$\frac{EI\alpha}{2R^3} \sum_{n=2,4,..}^{\infty} A_n^2 \left[1 - \left(\frac{n\pi}{2\alpha}\right)^2\right]^2 - \frac{RRm\alpha}{2} \sum_{n=2,4,..}^{\infty} A_n^2$$

$$- \frac{2RRm\alpha^3}{\pi^2} \sum_{n=2,4,..}^{\infty} \frac{A_n^2}{n^2} - RRm\alpha B^2 - \gamma\left[B - \frac{2\alpha}{\pi} \sum_{n=2,4,..}^{\infty} \frac{A_n}{n}\right]$$

which was minimized. For a one-term approximation to the resulting series frequency equation, Nelson expressed the nondimensional frequency parameter δ, as

$$\delta = R \frac{mL^4}{EI\pi^4}$$

where $L = 2R\alpha$, the developed length of the arch. The roots R_1, R_2, ... obtained from the minimizing process have the property that $R_1 \geq \omega_1^2$, $R_2 \geq \omega_2^2$, ...

Nelson referred to the phenomena of "frequency cross-over" by showing that the arch will shift from a one-node to a three-node mode of vibration by increasing the arch opening angle. Nelson observed that

this occurred at an opening angle of about 570 degrees.

Results were presented for arch opening angles beyond 360 degrees. However, in the theory, it was assumed that the arch was vibrating in its plane of initial curvature. To satisfy this assumption it is physically impossible to have an actual arch greater than 360 degrees. Hence, any results presented by Nelson for arch opening angles greater than 360 degrees have no physical significance.

Nelson also investigated symmetrical modes and extensional modes by using the above method of analysis. Graphical results were presented indicating for what arch parameters the inextensional theory yields accurate results and for what parameters the extensional theory must be used.

Lang (18, 1962; 19, 1963)

Except for Archer's transient solution for an arch when one support is given a particular displacement, the studies conducted thus far consisted of finding the natural frequencies and mode shapes for freely vibrating arches. It appears that Lang was the first to propose a closed form solution for arches or rings which are excited by time dependent external forces. A theoretical analysis was applied to both the extensional and inextensional case. The classical approach was used to derive the governing differential equations. For the extensional case, the homogeneous equation obtained was

$$V_n^{VI} + \left(2 + \frac{\lambda_n^2}{\left(\frac{R}{k}\right)^2}\right) V_n^{IV} + \left(1 - \lambda_n^2 - \frac{\lambda_n^2}{\left(\frac{R}{k}\right)^2}\right) V_n^{II} + \lambda_n^2 \left(1 - \frac{\lambda_n^2}{\left(\frac{R}{k}\right)^2}\right) V_n = 0 \qquad 1.2\text{-}24$$

where k is the radius of gyration of the cross-section and the terms $\lambda_n^2/(R/k)^2$ take into account the effects of stretching of the center line.

For the inextensional case, the complete governing differential equation obtained was

$$\frac{EI}{mR^4}\left[\frac{\partial^6 v}{\partial\phi^6} + 2\frac{\partial^4 v}{\partial\phi^4} + \frac{\partial^2 v}{\partial\phi^2}\right] + \frac{\partial^4 v}{\partial\phi^2\partial t^2}$$

$$-\frac{\partial^2 v}{\partial t^2} = \frac{1}{m}\left[\frac{\partial P_R(\phi,t)}{\partial\phi} - P_T(\phi,t)\right] \qquad 1.2\text{-}25$$

where P_R and P_T are external loads per unit arch length in the radial and tangential direction respectively. Also for the inextensional case, the radial displacement u and the tangential displacement v are related by the equation

$$\frac{\partial v}{\partial\phi} = u\ . \qquad 1.2\text{-}26$$

Since eq. 1.2-25 is a linear equation, the steady state solution Lang proposed was a series in terms of the free modes of vibration, i.e.

$$v_p(\phi,t) = \sum_{i=1}^{\infty} V_i(\phi)\ \eta_i(t) \qquad 1.2\text{-}27$$

where V_i is the i-th mode of free vibration in the tangential direction and $\eta_i(t)$ is a function of time, as yet unknown. Substituting eq. 1.2-27 into eq. 1.2-25, multiplying by $V_j d\phi$, and integrating between

$-\alpha$ and α, the resulting equation is

$$\sum_{i=1}^{\infty} [(\ddot{\eta}_i + \omega_i^2 \eta_i) \int_{-\alpha}^{\alpha} (V_i^I V_j^I + V_i V_j) d\phi] = - \int_{-\alpha}^{\alpha} \frac{V_j}{m} [\frac{\partial P_R}{\partial \phi} - P_T] d\phi, \qquad 1.2\text{-}28$$

where $(\ddot{\ })$ means $d^2(\ )/dt^2$, and $(\ )^I$, $(\ )^{II}$, ... means $d(\ )/d\phi$, $d^2(\ )/d\phi^2$, etc. The orthogonality condition for the free modes of vibration is

$$\int_{-\alpha}^{\alpha} (V_i^I V_j^I + V_i V_j) d\phi = 0 \text{ for } i \neq j$$

and for i = j the modes were normalized according to

$$\frac{1}{2\alpha} \int_{-\alpha}^{\alpha} (V_i^I V_j^I + V_i V_j) d\phi = 1 . \qquad 1.2\text{-}29$$

Because of the orthogonality condition, the i-th and the j-th modes uncoupled in eq. 1.2-28 and using eq. 1.2-29, the resulting equation for $\eta_j(t)$ was found to be

$$\ddot{\eta}_j + \omega_j^2 \eta_j = D_j(t) \qquad 1.2\text{-}30$$

where

$$D_j(t) = - \frac{\int_{-\alpha}^{\alpha} \frac{V_j}{m} (\frac{\partial P_R}{\partial \phi} - P_T) \, d\phi}{2\alpha} .$$

Lang obtained the steady state solution in integral form but did not

evaluate it for any particular type of external loads.

Experimental evaluation of the homogeneous solution to eq. 1.2-25 was obtained showing good agreement between theory and experiment for the natural frequencies and corresponding mode shapes for the first three symmetric, in-plane modes for a complete ring with a point clamping, i.e. the ring was essentially an arch with fixed ends and α = 180 degrees. No experimental verification was presented for other arches.

In a later report, Lang (19) tabulated the theoretical dimensionless frequency parameters as given by

$$\lambda_n^2 = \omega_n^2 \frac{mR^4}{EI}$$

and the corresponding mode shapes for the first five in-plane modes for arches with opening angles of 180 degrees for various types of boundary conditions.

Takahashi (20, 1963)

Lagrange's equation was used by Takahashi to obtain the governing differential equation for the vibration of a circular arch in its initial plane of curvature. This approach yielded

$$L = \frac{EI}{2R^3} \int_{-\alpha}^{\alpha} [\lambda_n^2(U_n^2+V_n^2) - (V_n^I + U_n^{II})^2 - (\frac{R}{k})^2 (V_n^I - U_n)^2] \, d\phi \, , \qquad 1.2\text{-}31$$

where sinusoidal time functions were assumed and L is the Lagrangian. The value of λ_n^2 is given by eq. 1.2-5. The method of calculus of variation was applied to eq. 1.2-31 and upon rearranging the resulting

equations the following equation was obtained

$$V_n^{VI} + \left(2 + \frac{\lambda_n^2}{(\frac{R}{k})^2}\right) V_n^{IV} + \left(1 - \lambda_n^2 - \frac{\lambda_n^2}{(\frac{R}{k})^2}\right) V_n^{II}$$

$$+ \lambda_n^2 \left(1 - \frac{\lambda_n^2}{(\frac{R}{k})^2}\right) V_n = 0 \, . \qquad 1.2\text{-}32$$

This equation is identical to the equation Lang obtained in his analysis (eq. 1.2-24). If arch parameters are chosen such that

$$\lambda_n^2 << (\frac{R}{k})^2$$

i.e. stretching of the mid-surface is negligible, eq. 1.2-32 reduces to the equation Lamb obtained (eq. 1.2-4). Takahashi's solution indicated that the slenderness ratio, $(R/k)^2$, influences the resonant frequencies for symmetric modes, however, this ratio has little effect on the frequencies for unsymmetrical modes. Takahashi also observed the "frequency cross-over" reported by Nelson (17).

Nelson (21, 1964)

Extending his earlier work (17), Nelson investigated the frequency cross-over between extensional and inextensional modes for pinned-end circular arches. Results were presented showing the effects of the parameter, $g = (L/k\pi)^4$, on the mode of vibration, where L is the developed length of the arch. These results indicated that for certain arch opening angles and certain values of g, the arch vibrated

in the extensional mode rather than in the inextensional mode. It was shown that there was a unique value of the frequency where this cross-over would occur which Nelson called the cross-over point.

Another aspect of Nelson's investigation involved finding over what range of α(α = one-half the arch opening angle) and for what values of g the inextensional theory can be used to obtain sufficiently accurate results.

Antman and Warner (22, 1965)

Starting with the basic equations as established by Love, Antman and Warner investigated the stability of vibrating arches. The governing equations were written as

$$\frac{\partial N}{\partial s} + \kappa \frac{\partial M}{\partial s} + \kappa M_0 + N_0 - m \frac{\partial^2 v}{\partial t^2} = 0 \qquad 1.2\text{-}33$$

and

$$\frac{\partial^2 M}{\partial s^2} + \frac{\partial M_0}{\partial s} - \kappa N - Q_0 + m \frac{\partial^2 u}{\partial t^2} = 0 \qquad 1.2\text{-}34$$

where M_0, N_0 and Q_0 are the externally applied moment, tangential load and shear load respectively per unit length of arch, κ is the deformed curvature and ds is an element of arch length. Antman and Warner argued that if the moment M, normal force N and curvature κ were expressed in terms of the displacements u and v, the term κN in eq. 1.2-34 gave rise to a nonlinear coupling in displacements. However, if N was regarded as a known function of s and t, then κN contributed a linear term to

eq. 1.2-34. Thus, these authors obtained an independent solution for N from the linear equations and substituted this value of N into eq. 1.2-34 which was then examined for stability. For a circular arch of radius R, the resulting equation was

$$\frac{EI}{R^4}\left(\frac{\partial^4 u}{\partial\phi^4} + \frac{\partial^2 u}{\partial\phi^2}\right) - \frac{N}{R^2}\left(\frac{\partial^2 u}{\partial\phi^2} + u\right) + m\frac{\partial^2 u}{\partial t^2} = \frac{N}{R} + Q_0 - \frac{1}{R}\frac{\partial M_0}{\partial\phi} \qquad 1.2\text{-}35$$

where N was obtained from

$$\frac{\partial^2 N}{\partial\phi^2} + N - \frac{mR^2}{EA}\frac{\partial^2 N}{\partial t^2} = -R\,Q_0 - R\frac{\partial N_0}{\partial\phi} + 2mR\frac{\partial^2 u}{\partial t^2} \qquad 1.2\text{-}36$$

for the extensional case and from

$$\frac{\partial^2 N}{\partial\phi^2} + N = -R\,Q_0 - R\frac{\partial N_0}{\partial\phi} + 2mR\frac{\partial^2 u}{\partial t^2} \qquad 1.2\text{-}37$$

for the inextensional case. Although N could be solved from eq. 1.2-36 or eq. 1.2-37, the authors obtained N by linearizing the governing differential equations by assuming a constant curvature before and after deformation and then solving for a steady state value of N using Lang's (18) approach. Denoting the steady state value of N by

$$N = N^*(\phi)\cos\Omega t$$

and substituting this value of N into eq. 1.2-35 the following equation

was obtained,

$$\frac{EI}{R^4}\left(\frac{\partial^4 u}{\partial\phi^4} + \frac{\partial^2 u}{\partial\phi^2}\right) - \frac{N^*(\phi)}{R^2}\cos\Omega t\left(\frac{\partial^2 u}{\partial\phi^2} + u\right) +$$

$$m\frac{\partial^2 u}{\partial t^2} = f(\phi)\cos\Omega t \qquad 1.2\text{-}38$$

where

$$f(\phi) = \frac{N^*(\phi)}{R} + Q_0^*(\phi) - \frac{1}{R}\frac{dM_0^*(\phi)}{d\phi}$$

and

$$Q_0 = Q_0^*(\phi)\cos\Omega t\ ,\ M_0 = M_0^*(\phi)\cos\Omega t\ .$$

The problem was now reduced to finding under what conditions the solution u to eq. 1.2-38 would remain bounded for all time, $t > 0$. Since eq. 1.2-38 was not separable, a Kantorovich's modification of Galerkin's method to reduce eq. 1.2-38 to a system of coupled Mathieu equations was employed.

Antman and Warner analyzed the stability of a semi-circular arch under radial forced end vibrations as shown in Fig. 1.2-2. From this investigation it was concluded that "secondary resonant frequencies" were given by

$$\frac{\pm\beta_i \pm\beta_k}{j}$$

where j is any integer, i may equal k and β_k^2 is defined as

$$\beta_k^2 = \frac{EI}{mR^2} (k+1)^2 [(k+1)^2 - 1] .$$

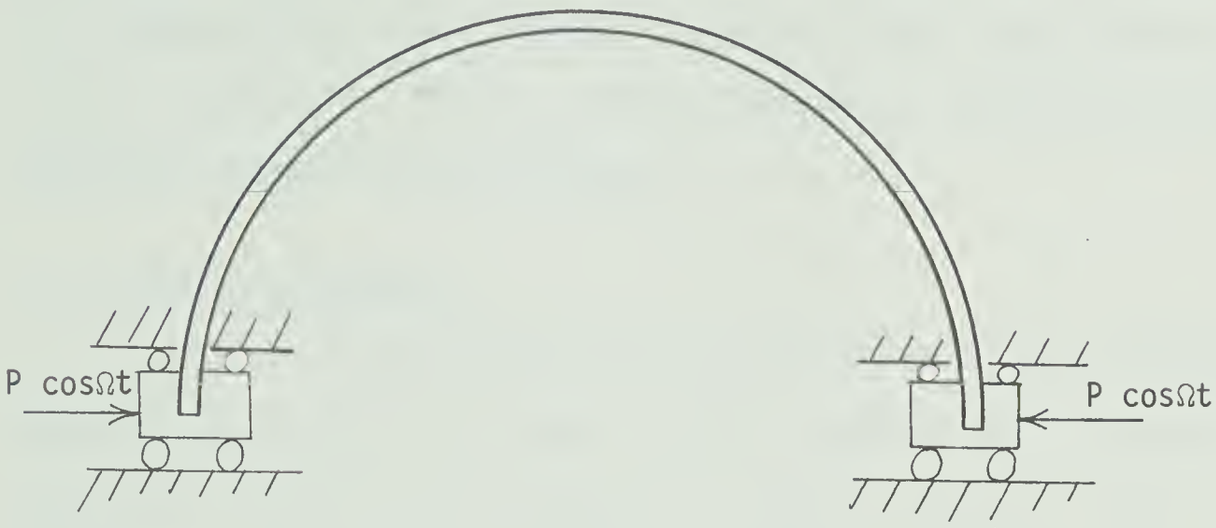

FIG. 1.2-2 ARCH MODEL USED BY ANTMAN AND WARNER

Popescu (27, 1970)

To investigate the dynamic stability of arches, Popescu used an energy method similar to that used by Bolotin to obtain the governing equation. The arches were assumed to be subjected to a distributed load q(t) given by the equation

$$q(t) = Q_0 + Q \cos \Omega t$$

where Q_0 is the static radial load, Q is the amplitude of the periodically variable load and Ω is the pulsating frequency. The governing equation was reduced to a Mathieu equation which was then analyzed for stability. In obtaining the expression for the kinetic energy, Popescu did not account for the tangential displacement of the arch. This resulted in a higher bound for the frequency of free vibration than that obtained by Den Hartog, Nelson, Eppink and Veletsos, and Bolotin who considered the tangential displacement.

1.3 Closure to Chapter I

The basic equation governing free vibrations of inextensible arches had been obtained by Lamb in 1888. Since that time, numerous approximate techniques were employed to obtain responses of deep arches. For example, Den Hartog used the Rayleigh quotient to obtain the characteristics of the first mode for both the extensional and inextensional case; Bolotin investigated the effects of parametric excitation and the effects of pulsating pressure loads on arches using the Galerkin method; Eppink and Veletsos obtained the dynamic response of arches excited by dynamic pressure loads by replacing the continuous arch with a framework of rigid bars and flexible joints; Nelson used the Rayleigh-Ritz method in conjunction with Lagrangian multipliers to calculate the characteristics of the free modes of vibration; Volterra and Morell extended the Rayleigh-Ritz method to include arches with center-lines other than circular; and Lang and Reed used the transfer matrix technique to solve for the free vibration characteristics.

Other investigators such as Archer, Morley, Love, Hoppe and

Takahashi solved the governing equation for arches or rings for free vibrations in closed form. Antman and Warner considered some nonlinear terms in the governing equations and performed a stability analysis for arches. It appears that Lang was the first investigator to derive the orthogonality condition for the free modes of vibration for an arch. Lang proposed a steady state solution as a series in terms of the free modes of vibration. This steady state solution was stated in integral form and was not evaluated for any type of loading.

Very little experimental data is available to evaluate the above approximate and closed form solutions. Lang conducted experimental tests on complete rings only, obtaining good agreement between theory and experiment for the natural frequencies and mode shapes. However, no experimental evaluation was provided for the steady state solution.

On the basis of the literature review, it is evident that an extension to the presently existing theory is necessary in order to provide a solution for the dynamic response of arches subjected to cyclic support movement. The theoretical analysis to the above problem is presented in Chapter II.

Chapter II

Theory

2.1 Derivation of the Governing Differential Equations

The governing differential equation used in this analysis will be derived by considering the equilibrium of an arch element. Lang's (18) approach for obtaining the steady state solution will be modified to account for the inertial loads caused by support movement. A steady state solution for symmetrical and unsymmetrical support movement will be proposed. The coordinate system used is shown in Fig. 1.1-1.

The assumptions used in the theory are:

1. The material is perfectly elastic and obeys Hooke's Law.

2. The displacements $u(\phi,t)$ and $v(\phi,t)$ measure deformation only, i.e. rigid body motion is not accounted for by u and v.

3. The mass per unit arch length m, thickness H, and width b are constant along the arch circumference.

4. Displacements out-of-the plane of initial arch curvature are not considered.

5. Although the existence of damping is acknowledged, it is assumed that its effects on the steady state solution are negligible.

6. The arch vibrates with no extension of the center line i.e. $(R/k)^2 >> \lambda_n^2$.

7. The undeformed shape of the arch is circular with radius R.

8. Radial displacements u are small such that $R \pm u \approx R$.

9. Rotatory inertia and shear deformation effects are small compared with the effects of flexure.

10. Second order terms are negligible when compared to first order terms.

By applying dynamic equilibrium to an element of an arch shown in Fig. 1.2-1, the three governing equations are:

$$\frac{\partial Q}{\partial \phi} + N - mR \frac{\partial^2 u}{\partial t^2} + R P_R = 0 , \qquad 2.1\text{-}1$$

$$\frac{\partial N}{\partial \phi} - Q - mR \frac{\partial^2 v}{\partial t^2} + R P_T = 0 , \qquad 2.1\text{-}2$$

and

$$\frac{1}{R} \frac{\partial M}{\partial \phi} = Q \qquad 2.1\text{-}3$$

where $P_T(\phi,t)$ and $P_R(\phi,t)$ represent the external load per unit arch length acting in the tangential and radial directions respectively. Combining eq. 2.1-1, 2.1-2 and 2.1-3 together with eq. 1.2-10 and 1.2-11 yields

$$\frac{EI}{mR^4} \left(\frac{\partial^5 u}{\partial \phi^5} + 2 \frac{\partial^3 u}{\partial \phi^3} + \frac{\partial u}{\partial \phi}\right) + \frac{\partial^3 u}{\partial \phi \partial t^2} - \frac{\partial^2 v}{\partial t^2} = \frac{1}{m} \left(\frac{\partial P_R}{\partial \phi} - P_T\right) . \qquad 2.1\text{-}4$$

The condition of inextensibility as given by eq. 1.2-12 separates eq.

2.1-4 into

$$\frac{EI}{mR^4}\left(\frac{\partial^6 v}{\partial\phi^6} + 2\frac{\partial^4 v}{\partial\phi^4} + \frac{\partial^2 v}{\partial\phi^2}\right) + \frac{\partial^4 v}{\partial\phi^2\partial t^2} - \frac{\partial^2 v}{\partial t^2} = \frac{1}{m}\left(\frac{\partial P_R}{\partial\phi} - P_T\right) \qquad 2.1\text{-}5$$

and

$$\frac{EI}{mR^4}\left(\frac{\partial^6 u}{\partial\phi^6} + 2\frac{\partial^4 u}{\partial\phi^4} + \frac{\partial^2 u}{\partial\phi^2}\right) + \frac{\partial^4 u}{\partial\phi^2\partial t^2} - \frac{\partial^2 u}{\partial t^2} = \frac{1}{m}\left(\frac{\partial^2 P_R}{\partial\phi^2} - \frac{\partial P_T}{\partial\phi}\right) \qquad 2.1\text{-}6$$

It will be shown that eq. 2.1-6 reduces to the governing equation of a straight beam in the limit as $R \to \infty$. Rewriting eq. 2.1-6 using an element of arch length ds as the independent variable where $Rd\phi = ds$, yields

$$\frac{EI}{m}\left(\frac{\partial^6 u}{\partial s^6} + \frac{1}{R^2}\frac{\partial^4 u}{\partial s^4} + \frac{1}{R^4}\frac{\partial^2 u}{\partial s^2}\right) + \frac{\partial^4 u}{\partial s^2\partial t^2} - \frac{1}{R^2}\frac{\partial^2 u}{\partial t^2} = \frac{1}{m}\left(\frac{\partial^2 P_R}{\partial s^2} - \frac{1}{R}\frac{\partial P_T}{\partial s}\right) . \qquad 2.1\text{-}7$$

Taking the limit of eq. 2.1-7 as $R \to \infty$ and integrating the resulting equation twice with respect to ds yields

$$\frac{EI}{m}\frac{\partial^4 u}{\partial s^4} + \frac{\partial^2 u}{\partial t^2} = \frac{1}{m}P_R , \qquad 2.1\text{-}8$$

where the integration time functions are omitted. Equation 2.1-8 is the governing equation for the flexural response of a straight beam.

2.2 Solution to the Homogeneous Equation

The homogeneous equation can be written as

$$\frac{EI}{mR^4}\left(\frac{\partial^6 w}{\partial\phi^6} + 2\frac{\partial^4 w}{\partial\phi^4} + \frac{\partial^2 w}{\partial\phi^2}\right) + \frac{\partial^4 w}{\partial\phi^2\partial t^2} - \frac{\partial^2 w}{\partial t^2} = 0 \qquad 2.2\text{-}1$$

where $w(\phi,t)$ represents either $v(\phi,t)$ or $u(\phi,t)$. Assuming a solution of the form

$$w(\phi,t) = \sum_{n=1}^{\infty} W_n(\phi)\, T_n(t) \qquad 2.2\text{-}2$$

separates eq. 2.2-1 into

$$W_n^{VI} + 2W^{IV} + (1-\lambda_n^2)\, W_n^{II} + \lambda_n^2 W_n = 0 \qquad 2.2\text{-}3$$

and

$$\ddot{T}_n + \omega_n^2 T_n = 0\ , \qquad 2.2\text{-}4$$

where

$$\lambda_n^2 = \omega_n^2 \frac{mR^4}{EI} \qquad 2.2\text{-}5$$

and

$$\frac{d(\ )}{d\phi} = (\ )^I\ ,\ \frac{d(\ )}{dt} = (\dot{\ })\ ,\ \text{etc.}$$

The solution to eq. 2.2-4 is

$$T_n = A_n e^{i\omega_n t} . \qquad 2.2\text{-}6$$

Since eq. 2.2-3 is an ordinary differential equation with constant coefficients a solution of the form

$$W_n(\phi) = \sum_{j=1}^{6} C_{nj} e^{r_{nj}\phi} \qquad 2.2\text{-}7$$

can be assumed. Substituting eq. 2.2-7 into eq. 2.2-3 yields an auxiliary equation

$$r_n^6 + 2r_n^4 + r_n^2 (1-\lambda_n^2) + \lambda_n^2 = 0 . \qquad 2.2\text{-}8$$

Equation 2.2-8 is a cubic equation in r_n^2 and applying the standard algebraic solution for cubic equations (Sokolnikoff (23)) a solution for r_n^2 is obtained. By considering the discriminant of the cubic equation, it was found that for $0 < \lambda_n^2 < 0.113$, the solution to eq. 2.2-3 can be expressed as

$$W_n(\phi) = C_{n1} \cos \nu_1\phi + C_{n2} \sin \nu_1\phi + C_{n3} \cos \nu_2\phi$$

$$+ C_{n4} \sin \nu_2\phi + C_{n5} \cos \nu_3\phi + C_{n6} \sin \nu_3\phi \qquad 2.2\text{-}9$$

where $r_{n(1,2)} = \pm i\nu_1$, $r_{n(3,4)} = \pm i\nu_2$ and $r_{n(5,6)} = \pm i\nu_3$ and the $r_{n(j)}$'s, j = 1, 2, ...6 are the roots of eq. 2.2-8. Similarly for $0.113 < \lambda_n^2 < 17.64$ the solution is

$$W_n(\phi) = C_{n1} \cos \nu_1\phi + C_{n2} \sin \nu_1\phi + C_{n3} \cos \nu_2\phi \cosh \mu_2\phi$$

$$+ C_{n4} \cos \nu_2\phi \sinh \mu_2\phi + C_{n5} \sin \nu_2\phi \cosh \mu_2\phi + C_{n6} \sin \nu_2\phi \sinh \mu_2\phi$$

2.2-10

where $r_{n(1,2)} = \pm i\nu_1$, $r_{n(3,4)} = \pm \mu_2 \pm i\nu_2$ and $r_{n(5,6)} = \pm \mu_2 \mp i\nu_2$. For $\lambda_n^2 > 17.64$ the solution is

$$W_n(\phi) = C_{n1} \cos \nu_1\phi + C_{n2} \sin \nu_1\phi + C_{n3} \cosh \mu_1\phi$$

$$+ C_{n4} \sinh \mu_1\phi + C_{n5} \cosh \mu_2\phi + C_{n6} \sinh \mu_2\phi \qquad 2.2\text{-}11$$

where $r_{n(1,2)} = \pm i\nu_1$, $r_{n(3,4)} = \pm \mu_1$ and $r_{n(5,6)} = \pm \mu_2$. The constants C_{nj} , $j = 1,2,\ldots 6$ are determined from the boundary conditions. Equations 2.2-9, 2.2-10 and 2.2-11 are the solutions to the homogeneous eq. 2.2-3 where $W_n(\phi)$ represents either $V_n(\phi)$ or $U_n(\phi)$ depending whether the tangential or radial mode shapes are considered. Before a particular solution to eq. 2.1-5 and 2.1-6 can be evaluated, the orthogonality condition for the free modes of vibrations must be found.

2.3 Orthogonality Condition

To evaluate the orthogonality condition, consider eq. 2.2-3 where $W_n(\phi)$ is replaced by $V_n(\phi)$

$$V_n^{VI} + 2 V_n^{IV} + (1-\lambda_n^2) V_n^{II} + \lambda_n^2 V_n = 0 . \qquad 2.3\text{-}1$$

Multiplying eq. 2.3-1 through by $V_m\, d\phi$ and integrating between the limits of $-\alpha$ to α yields

$$B_1 - \int_{-\alpha}^{\alpha} (V_n^{III} V_m^{III} - 2\, V_n^{II} V_m^{II} + V_n^{I} V_m^{I})\, d\phi =$$

$$- \lambda_n^2 \int_{-\alpha}^{\alpha} (V_n^{I} V_m^{I} + V_n V_m)\, d\phi \qquad 2.3\text{-}2$$

where

$$B_1 = [V_n^{V} V_m - V_n^{IV} V_m^{I} + V_n^{III} V_m^{II} + 2\, V_n^{III}\, V_m$$

$$- 2\, V_n^{II} V_m^{I} + (1-\lambda_n^2)\, V_n^{I} V_m]_{-\alpha}^{\alpha} .$$

The constant B_1 can be evaluated after the boundary conditions at $\phi = \pm \alpha$ are specified. Another equation similar to eq. 2.3-2 can be obtained by interchanging subscripts m and n. This yields

$$B_2 - \int_{-\alpha}^{\alpha} (V_m^{III} V_n^{III} - 2\, V_m^{II} V_n^{II} + V_m^{I} V_n^{I})\, d\phi =$$

$$- \lambda_m^2 \int_{-\alpha}^{\alpha} (V_m^{I} V_n^{I} + V_m V_n)\, d\phi \qquad 2.3\text{-}3$$

where

$$B_2 = [V_m^{V} V_n - V_m^{IV} V_n^{I} + V_m^{III} V_n^{II} + 2\, V_m^{III} V_n$$

$$- 2\, V_m^{II} V_n^{I} + (1-\lambda_n^2)\, V_m^{I} V_n]_{-\alpha}^{\alpha} .$$

Subtracting eq. 2.3-3 from eq. 2.3-2 yields

$$B_1 - B_2 = (\lambda_m^2 - \lambda_n^2) \int_{-\alpha}^{\alpha} (V_n^I V_m^I + V_n V_m)\, d\phi. \qquad 2.3\text{-}4$$

When pinned-end, clamped-end or free-end boundary conditions are applied and B_1 and B_2 are evaluated, it is found that the left-hand side of eq. 2.3-4 is identically zero. Equation 2.3-4 can be written as

$$(\lambda_m^2 - \lambda_n^2) \int_{-\alpha}^{\alpha} (V_n^I V_m^I + V_n V_m)\, d\phi = 0 \,. \qquad 2.3\text{-}5$$

Hence, for $m \neq n$,

$$\int_{-\alpha}^{\alpha} (V_n^I V_m^I + V_n V_m)\, d\phi = 0 \,, \qquad 2.3\text{-}6$$

and for $m = n$, the eigenvectors are normalized such that

$$\frac{1}{2\alpha} \int_{-\alpha}^{\alpha} (V_m^I V_m^I + V_m V_m)\, d\phi = 1 \qquad 2.3\text{-}7$$

Using the orthogonal condition as given by eq. 2.3-6 and the normalization given by eq. 2.3-7, the steady state solution to eq. 2.1-5 and 2.1-6 can be evaluated.

2.4 Steady State Solution

The steady state solution to eq. 2.1-5 can be assumed to be

$$v_p(\phi,t) = \sum_{j=1}^{\infty} V_j(\phi)\, \eta_j(t) \qquad 2.4\text{-}1$$

where V_j is the j-th free mode of vibration and η_j is a function as yet undetermined. Substituting eq. 2.4-1 into eq. 2.1-5 yields

$$\sum_{j=1}^{\infty} \left[\frac{EI}{mR^4} \left(V_j^{VI} + 2\, V_j^{IV} + V_j^{II}\right) \eta_j + \ddot{\eta}_j \left(V_j^{II} - V_j\right)\right]$$

$$= \frac{1}{m} \left(\frac{\partial P_R}{\partial \phi} - P_T\right) . \qquad 2.4\text{-}2$$

Using eq. 2.3-1, eq. 2.4-2 can be reduced to

$$\sum_{j=1}^{\infty} \left[\left(V_j^{II} - V_j\right)\left(\ddot{\eta}_j + \omega_j^2 \eta_j\right)\right] = - \frac{1}{m} \left(\frac{\partial P_R}{\partial \phi} - P_T\right) . \qquad 2.4\text{-}3$$

Multiplying eq. 2.4-3 through by $V_k\, d\phi$ and integrating between the limits of $-\alpha$ to α yields

$$\sum_{j=1}^{\infty} \left[\left(\ddot{\eta}_j + \omega_j^2 \eta_j\right) \int_{-\alpha}^{\alpha} \left(V_j^I V_k^I + V_j V_k\right) d\phi\right] =$$

$$- \int_{-\alpha}^{\alpha} \frac{V_k}{m} \left(\frac{\partial P_R}{\partial \phi} - P_T\right) d\phi . \qquad 2.4\text{-}4$$

Applying the orthogonality condition as given by eq. 2.3-6 uncouples eq. 2.4-4 and then using the normalization as given by eq. 2.3-7, eq. 2.4-4 can be written as

$$\ddot{\eta}_k + \omega_k^2 \eta_k = D_k(t) \qquad 2.4\text{-}5$$

where

$$D_k(t) = -\frac{1}{2\alpha}\int_{-\alpha}^{\alpha}\frac{V_k}{m}\left(\frac{\partial P_R}{\partial \phi} - P_T\right) d\phi \ . \qquad 2.4\text{-}6$$

The solution to eq. 2.4-5 can be expressed in integral form as

$$n_k(t) = c'_{k1}\sin\omega_k t + c'_{k2}\cos\omega_k t + \frac{1}{\omega_k}\int_0^t D_k(\tau)\sin\omega_k(t-\tau)\,d\tau \qquad 2.4\text{-}7$$

where c'_{k1} and c'_{k2} are determined from the initial conditions of the arch.

The steady state solution for the tangential displacements is obtained by substituting eq. 2.4-7 into eq. 2.4-1. The steady state solution for the radial displacements can be obtained in a manner similar to that above, however, it can be done more simply by using the in-extensibility condition as given by eq. 1.2-12.

Steady state solutions are presented for two types of support movement. The motions will be defined by "symmetrically excited arches" for the one case and "unsymmetrically excited arches" for the second case.

2.5 Solution for Symmetrical Excitation

The term "symmetrical excitation" is taken to mean that both supports A and B, in Fig. 2.5-1, are vibrating in-phase and in the plane

of the initial curvature of the arch. Both supports have displacements whose direction is parallel to the line $\phi = 0$.

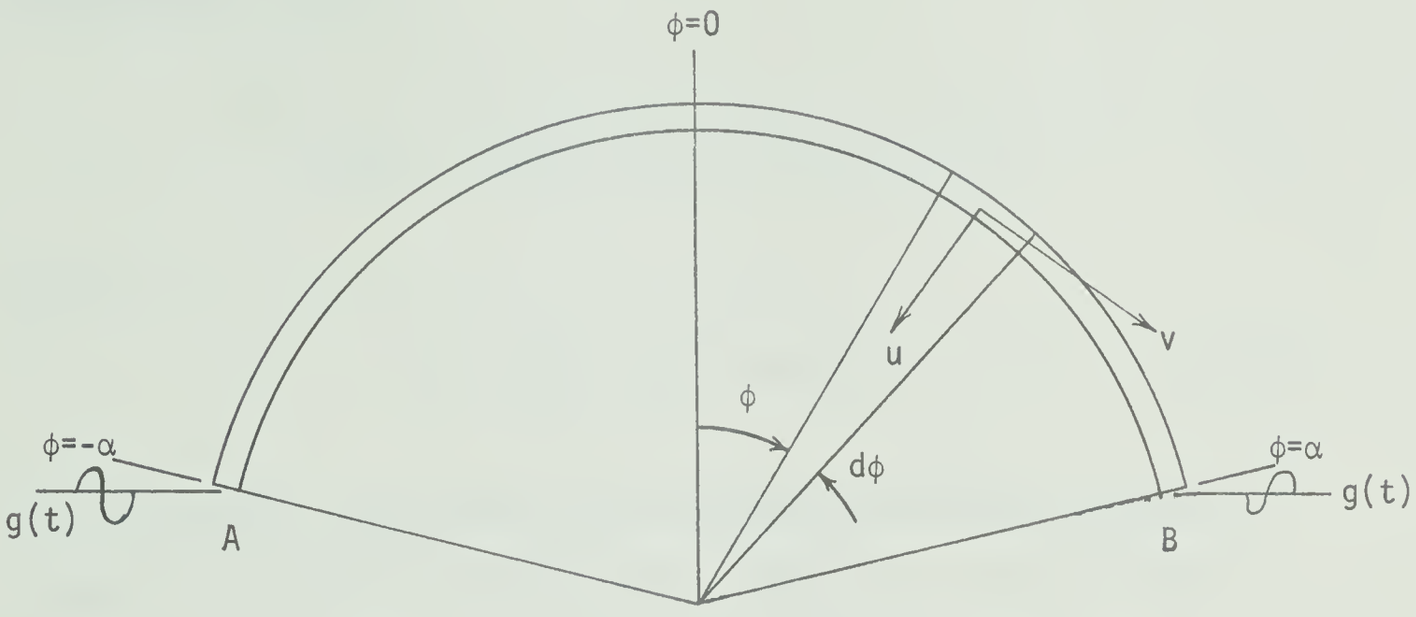

FIG. 2.5-1 MODEL FOR SYMMETRICAL EXCITATION

Let the function describing the support movement be denoted by g(t) where g(t) is twice continuously differentiable. Under this type of excitation the external forces P_T and P_R are

$$P_T = - m \ddot{g}(t) \sin \phi \qquad 2.5\text{-}1$$

and

$$P_R = - m \ddot{g}(t) \cos \phi. \qquad 2.5\text{-}2$$

Substituting eq. 2.5-1 and 2.5-2 into eq. 2.4-6 and from eq. 2.4-7 the solution for $\eta_k(t)$ is

$$\eta_k(t) = - \frac{1}{\omega_k} \int_0^t D_k' \ddot{g}(\tau) \sin \omega_k(t-\tau) \, d\tau \qquad 2.5\text{-}3$$

where

$$D_k' = \frac{1}{\alpha} \int_{-\alpha}^{\alpha} V_k(\phi) \sin \phi \, d\phi \qquad 2.5\text{-}4$$

and the initial conditions can be disregarded since some damping is present in an actual arch which will eliminate any initial effects leaving only the steady state terms. If g(t) is assumed to be

$$g(t) = G \sin \Omega t \, , \qquad 2.5\text{-}5$$

the solution for $\eta_k(t)$ becomes

$$\eta_k(t) = \frac{G \Omega^2 D_k'}{\omega_k^2 - \Omega^2} \sin \Omega t \, . \qquad 2.5\text{-}6$$

Substituting eq. 2.5-6 into eq. 2.4-1, the steady state solution for the tangential displacement becomes

$$\frac{v_p}{G} = \sum_{j=1}^{\infty} \frac{\Omega^2 D_j' V_j}{(\omega_j^2 - \Omega^2)} \sin \Omega t \qquad 2.5\text{-}7$$

and using eq. 1.2-12, the radial displacement is

$$\frac{u_p}{G} = \sum_{j=1}^{\infty} \frac{\Omega^2 D_j' U_j}{(\omega_j - \Omega^2)} \sin \Omega t \qquad 2.5\text{-}8$$

where the subscript p means steady state solution.

The terms v_p/G and u_p/G are referred to as magnificiation ratios in the tangential and radial directions respectively.

2.6 Solution for Unsymmetrical Excitation

With reference to Fig. 2.6-1, "unsymmetrical excitation" is taken to mean that support A is stationary and support B is vibrating in the plane of the initial arch curvature. The displacement of B is along a line parallel to the line $\phi = 0$.

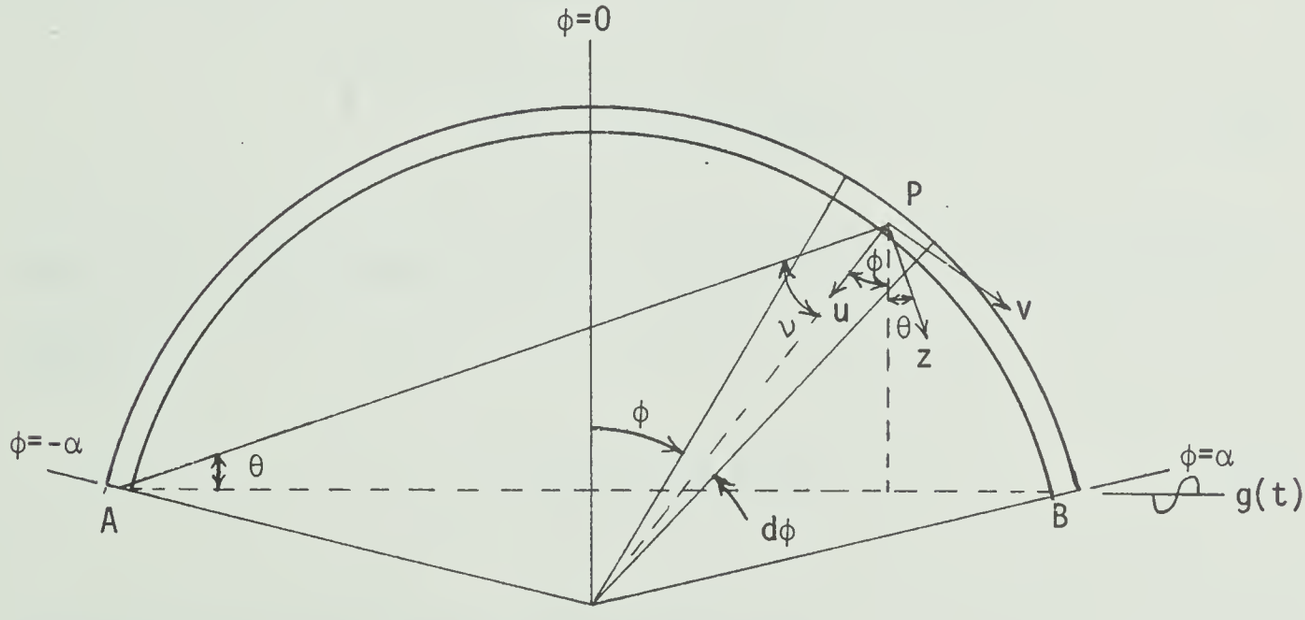

FIG. 2.6-1 MODEL FOR UNSYMMETRICAL EXCITATION

Assume the function describing the support movement is given by g(t) where g(t) is twice continuously differentiable. Let $\xi(t)$ define the rotation of the arch about support A due to the movement of support B. Point P is an arbitrarily chosen point on the circumference of the arch. If the amplitude of g(t) is small compared with the distance $\overline{AB}$, the rotation of the arch is given by

$$\xi(t) = \frac{g(t)}{\overline{AB}}$$

or by

$$\xi(t) = \frac{g(t)}{2R \sin \alpha} \qquad 2.6\text{-}1$$

since $\overline{AB} = 2R \sin \alpha$. The distance $\overline{AP}$ can be expressed as

$$\overline{AP} = 2R \sin \frac{1}{2} (\phi+\alpha) \ , \qquad 2.6\text{-}2$$

hence, the displacement of point P (represented by z in Fig. 2.6-1) is given by

$$z(\phi,t) = \overline{AP}\ \xi(t) \ . \qquad 2.6\text{-}3$$

The external forces P_T and P_R are given by

$$P_T = - m\ \overline{AP} \sin (\theta+\phi)\ \ddot{\xi} \qquad 2.6\text{-}4$$

and

$$P_R = - m \overline{AP} \cos (\theta+\phi) \ddot{\xi} \qquad 2.6\text{-}5$$

where

$$\theta = \frac{1}{2} (\alpha-\phi) .$$

Substituting for $\overline{AP}$, θ and $\ddot{\xi}$ in eq. 2.6-4 and 2.6-5 yields

$$P_T = - \frac{m \ddot{g}}{2 \sin \alpha} [1 - \cos (\phi+\alpha)] \qquad 2.6\text{-}6$$

and

$$P_R = - \frac{m \ddot{g}}{2 \sin \alpha} \sin (\phi+\alpha) . \qquad 2.6\text{-}7$$

Substituting eq. 2.6-6 and 2.6-7 into eq. 2.4-6, yields

$$D_k(t) = - \frac{\ddot{g}(t)}{4\alpha \sin \alpha} \int_{-\alpha}^{\alpha} V_k [1 - 2 \cos (\phi+\alpha)] d\phi,$$

and from eq. 2.4-7 $\eta_k(t)$ becomes

$$\eta_k(t) = c'_{k1} \sin \omega_k t + c'_{k2} \cos \omega_k t$$

$$- \frac{1}{\omega_k} \int_0^t \ddot{g}(\tau) D'_k \sin \omega_k (t-\tau) d\tau \qquad 2.6\text{-}8$$

where

$$D'_k = \frac{1}{4\alpha \sin\alpha} \int_{-\alpha}^{\alpha} V_k [1 - 2 \cos (\phi+\alpha)] d\phi \qquad 2.6\text{-}9$$

Substituting the assumed sinusoidal function for g(t) as given by eq. 2.5-5 into eq. 2.6-8, $\eta_k(t)$ can be written as

$$\eta_k(t) = \frac{G\ \Omega^2\ D_k'}{\omega_k^2 - \Omega^2} \sin \Omega t \qquad 2.6\text{-}10$$

where the initial conditions are disregarded due to the presence of some damping in a physical arch. When eq. 2.6-10 is substituted into eq. 2.4-1, the steady state solution for the tangential displacement is

$$\frac{v_p(\phi,t)}{G} = \sum_{j=1}^{\infty} \frac{\Omega^2\ D_j'\ V_j(\phi)}{(\omega_j^2 - \Omega^2)} \sin \Omega t \qquad 2.6\text{-}11$$

and using eq. 1.2-12, the steady state solution for the radial displacement is

$$\frac{u_p(\phi,t)}{G} = \sum_{j=1}^{\infty} \frac{\Omega^2\ D_j'\ U_j(\phi)}{(\omega_j^2 - \Omega^2)} \sin \Omega t\ , \qquad 2.6\text{-}12$$

where the subscript p denotes the steady state solution. Similarly as was defined for the symmetrical case, the terms u_p/G and v_p/G are referred to as magnification ratios in the radial and tangential directions respectively.

2.7 Computer Evaluation of Theoretical Solutions

The theoretical solutions were evaluated, only for pinned-end boundary conditions, using a digital computer. The boundary conditions were applied to the homogeneous solution as given by eq. 2.2-9, 2.2-10

or by 2.2-11 and the constants C_{nj}, n = mode number and j = 1,2,...6, were evaluated. The pinned-end boundary conditions, i.e. u = 0, v = 0 and M = 0 at $\phi = \pm \alpha$, are homogeneous and application of these to eq. 2.2-9, 2.2-10 or 2.2-11 results in six homogeneous algebraic equations. In order that a non-trivial solution for this set of equations exist, the determinant of the coefficients, which contains the natural frequency parameter $\lambda_n = \omega_n R^2 \sqrt{m/EI}$, must be zero. Since it was a difficult task to obtain an exact solution for λ_n by expanding and solving the six by six determinant, an iterative procedure was used. The procedure was started by assuming a value for λ_n which made the determinant negative and assuming another λ_n which made the determinant positive. An intermediate value for λ_n was then calculated and the determinant evaluated again. This procedure was continued until the determinant was zero or until the value of λ_n was iterated to 16 significant figures (capacity of the computer). It was not known before hand to which mode the particular value of λ_n would correspond; however, the mode was identified when the mode shape was evaluated. In the iterative process, it was possible to have the resulting determinant approach zero for the lower modes, however for the higher modes a small change in the value of λ_n (i.e. a change in the 16th significant figure) produced large changes in the value of the determinant. For example, for an arch having $\alpha \approx 100°$, a change by one in the 16th significant figure for λ_9 caused the value of the determinant to change from $\approx 10^{10}$ to $\approx -10^{10}$. However, for the same arch it was possible to iterate for

λ_1 such that the value of the determinant was $\approx 10^{-13}$. The value of the determinant was not zero for the higher modes, but because of the large oscillations in the value of the determinant for small changes in λ_n, it was decided that the iterative method evaluated the λ_n's with sufficient accuracy.

To aid in selecting the initial values of λ_n for the iterative process for arches with various α values, a plot, Fig. 2.7-1, was made of λ_n versus α for the first nine modes of free vibrations for pinned-end boundary conditions. A similar plot for fixed-end boundary conditions is shown in Fig. 2.7-2.

A comparison can be made of the values of λ_n obtained by the present theory and those obtained by Den Hartog (2), Eppink and Veletsos (10) and Nelson (17,21) who used approximate methods. As mentioned previously, an error was noted in the formula Den Hartog derived for λ_1 when displacements in the form of a polynomial were assumed. In Table 2.7-1, results are presented for λ_1 as obtained using the present theory, using Den Hartog's tabulated values, using the sinusoidal displacements and the equation derived by Den Hartog, and using the polynomial displacements assumed by Den Hartog and the corrected formula (i.e. $\lambda_1 = 1/\alpha^2[(\alpha^4 + 79.20\,\alpha^2 + 1584)/(1 + 0.07769\,\alpha^2)]^{1/2}$ for λ_1. As expected, the values Den Hartog obtained using the Rayleigh quotient are higher or equal to the values given by the present theory.

Eppink and Veletsos presented values only for one arch which had $\alpha = 43.6$ degrees. Results were presented when the arch was approximated by different number of bars. On the basis of this data, arches

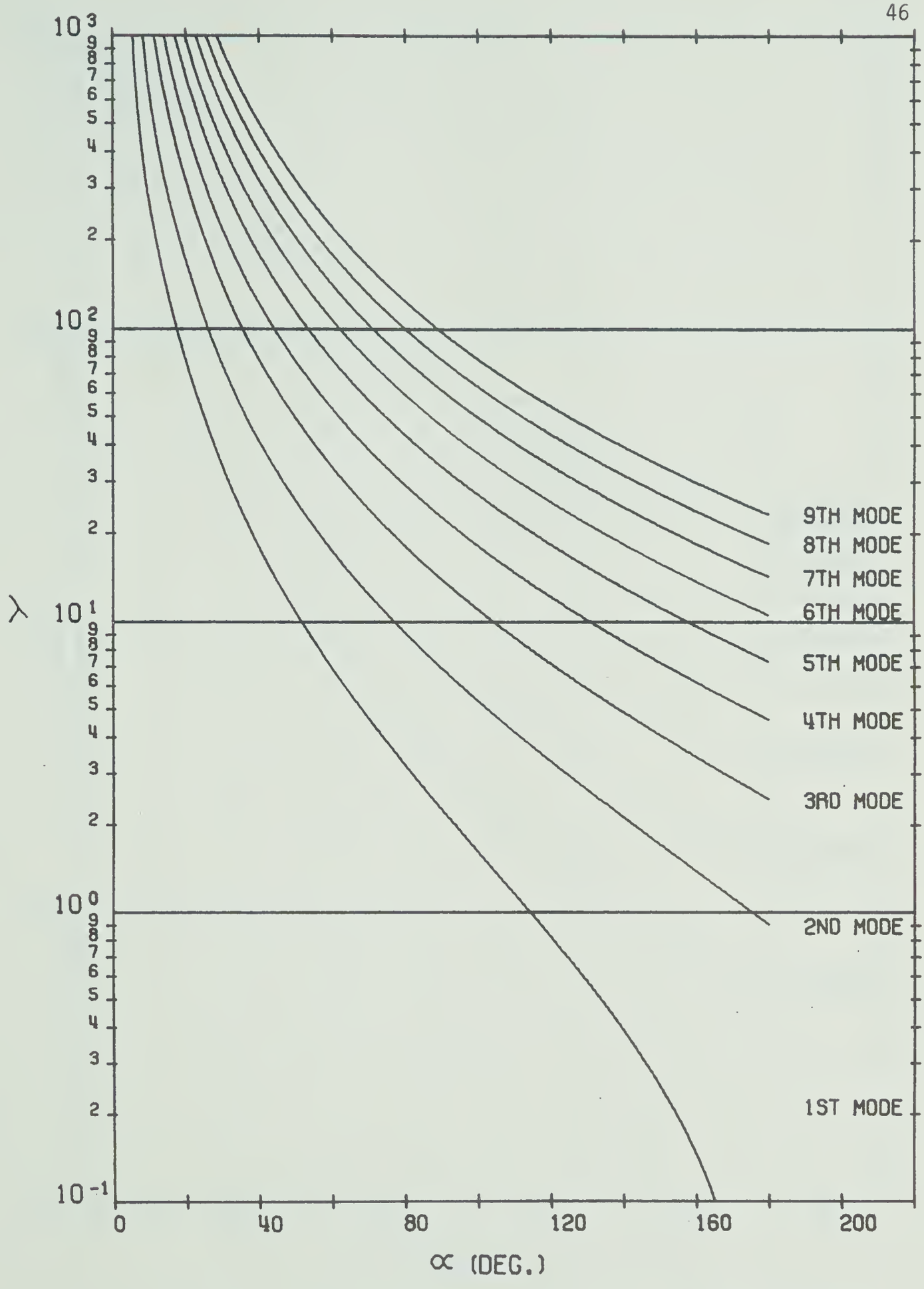

FIG. 2.7-1 DIMENSIONLESS NATURAL FREQUENCY; PINNED-END BOUNDARY CONDITION

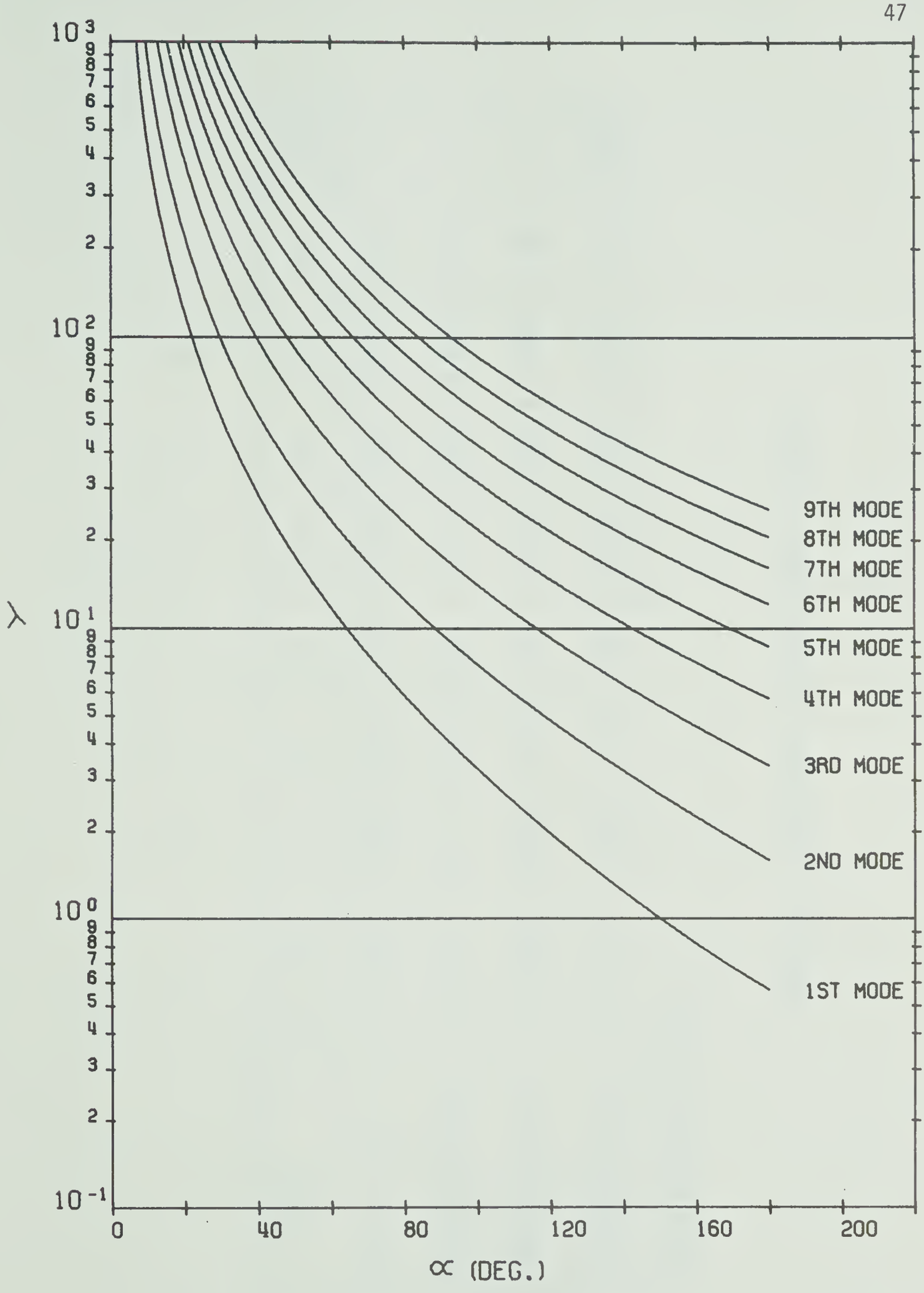

FIG. 2.7-2 DIMENSIONLESS NATURAL FREQUENCY; FIXED-END BOUNDARY CONDITION

α,Deg	0	20	40	60	80	100	120	140	160	180
Present Theory	∞	78.558	17.964	6.927	3.218	1.613	0.818	0.389	0.145	0
Den Hartog's Tabulated Values	∞	78.5	17.8	6.80	3.14	1.56	0.796	0.386	0.145	0
Den Hartog's Sinusoidal Disp.	∞	78.558	17.965	6.928	3.219	1.614	0.818	0.389	0.145	0
*Den Hartog's Polynomial Disp.	∞	79.179	18.098	6.977	3.243	1.630	0.831	0.412	0.161	0.050

*Using Corrected Formula

TABLE 2.7-1 COMPARISON WITH DEN HARTOG'S RESULTS

approximated by less bars gave lower values for the natural frequencies than those approximated by a larger number of bars, which indicates that this method yields lower bounds for the natural frequency. On the basis of a 20 bar approximation, the values for λ_n, n = 1,2,...9 and the values obtained from the present theory are shown in Table 2.7-2 for an arch with α = 43.6 degrees.

λ_n	λ_1	λ_2	λ_3	λ_4	λ_5	λ_6	λ_7	λ_8	λ_9
*Eppink & Veletsos's Results	14.8	36.4	65.8	103.1	150.9	205.1	269.6	340.1	420.6
Present Theory	14.8	34.6	65.8	102.9	151.0	205.1	270.4	341.5	423.8

* Results for a 20-bar approximation

TABLE 2.7-2 COMPARISON WITH EPPINK AND VELETSOS'S RESULTS

From Table 2.7-2, Eppink and Veletsos obtained the same or lower values for λ_n in all cases except when n = 2 and n = 4. No explanation, other than round off error, can be given for this.

A comparison with the values Nelson calculated for the first four modes is shown in Table 2.7-3. It should be noted that Nelson's values were obtained from a graph and may not be accurate to the number of significant figures listed. As expected, Nelson obtained larger values for the λ_n's using the Rayleigh-Ritz technique in conjunction

with Lagrangian multipliers than those obtained from the closed form solution.

λ \ α,Deg	*	0	45	90	135	180
λ_1	N	∞	13.8	2.27	0.474	0
	T	∞	13.764	2.267	0.474	0
λ_2	N	∞	32.5	6.93	2.39	0.901
	T	∞	32.404	6.923	2.366	0.901
λ_3	N	∞	62.0	14.1	5.44	2.46
	T	∞	61.673	13.978	5.349	2.447
λ_4	N	∞	97.8	23.3	9.32	4.61
	T	∞	96.446	22.820	9.267	4.597

*N - Nelson's values, obtained from graph
T - Values obtained from present theory

TABLE 2.7-3 COMPARISON WITH NELSON'S RESULTS

Since the agreement between the values of λ_n for the present theory and those of previous investigators is favourable, it can be assumed that the iterative method used in evaluating λ_n is sufficiently accurate. After the values of λ_n were evaluated, C_{nj}'s were calculated using the "least squares method". For example, suppose the original system of equations were defined by

$$\sum_{j,i=1}^{6} C_{nj} A_{ij} (\lambda_n) = 0 , \qquad 2.7\text{-}1$$

where n equals the mode number and the A_{ij}'s are constants which are evaluated when λ_n's are known. Dividing eq. 2.7-1 by $C_{nk} \neq 0$, $1 \leq k \leq 6$, results in five unknown ratios and 6 nonhomogeneous equations which are inconsistent since the exact value of λ_n is not known. The resulting equation is

$$\sum_{\substack{j,i=1 \\ j\neq k}}^{6} \left[\frac{C_{nj}}{C_{nk}} A_{ij}(\lambda_n) + A_{ik}(\lambda_n)\right] = 0 . \qquad 2.7\text{-}2$$

Equation 2.7-2 was reduced to five equations by defining a new function

$$\varepsilon = \left\{ \sum_{\substack{i,j=1 \\ j\neq k}}^{6} \left[\frac{C_{nj}}{C_{nk}} A_{ij}(\lambda_n) + A_{ik}(\lambda_n)\right]\right\}^2$$

and then minimizing ε with respect to each of the five ratios C_{nj}/C_{nk}. The ratios were then evaluated by solving simultaneously the resulting five equations. Equation 2.3-7 was used to solve for C_{nk}.

When the λ_n's, U_n's and V_n's were known, the steady state solution for radial displacements, as given by eq. 2.5-8 for symmetrical excitation, and by eq. 2.6-12 for unsymmetrical excitation was evaluated. For pinned-end boundary conditions, it was observed that if steady state solutions were required near the fourth mode it was sufficient to use eight terms in the series to obtain an accuracy to three significant figures. Better accuracy was obtained for forcing frequencies below the fourth natural frequency when an eight term series was used.

2.8 Closure to Chapter II

A theory has been presented which can be used to evaluate the dynamic response of thin circular arches subjected to inertial loads caused by cyclic support movement. The arch was assumed to be inextensible, radial displacements were small such that $R \pm u \approx R$, effects of damping on the steady state solution were assumed to be negligible, displacements were due to flexural effects only and the displacements were in the initial plane of the arch curvature. The orthogonality condition for the free modes of vibration was found which was used in the evaluation of the steady state solution. Steady state solutions were evaluated for both symmetrical and unsymmetrical excitations. For forcing frequencies near the fourth mode, an eight-term series in terms of the free modes of vibration, yielded the steady state solution accurate to three significant figures.

Since experimental results will only be presented for pinned-end arches, the theory has been evaluated in detail for these boundary conditions. Details of the experimental procedure are given in Chapter III.

Chapter III

Experimental Procedure

3.1 Description of Testing Equipment and Arches

The arches were excited by an Unholtz-Dickie, Model No. 100 Electrodynamic Shaker Table, capable of generating a maximum force of 225 pounds. The magnitude of the sinusoidal displacement and the frequency of excitation were controlled by a Brüel & Kjaer Model No. 11019 Automatic Vibration Exciter Control. With this equipment any desired frequency and displacement could be obtained, within the limitations of the apparatus. The frequency was measured by a General Radio Model No. 1150-AP Digital Frequency Meter having an accuracy of plus or minus one count. During testing, the frequency was recorded continuously on a General Radio Data Printer Model No. 1137-A in order to determine whether drifting of the frequency occurred during a test. The amplitude of displacement for the support and that of the arches were measured by micrometer probes, shown in Fig. 3.1-1. The probes were fitted with spring loaded tips to reduce any disturbances that might be induced when contact was made with the arch or support. The probe measuring the radial arch displacement was mounted on a movable arm permitting the rotation of the probe into any desired position. A simple electrical circuit was used to indicate when the probe made contact with the arch. A photographic view of the testing equipment is shown in Fig. 3.1-2.

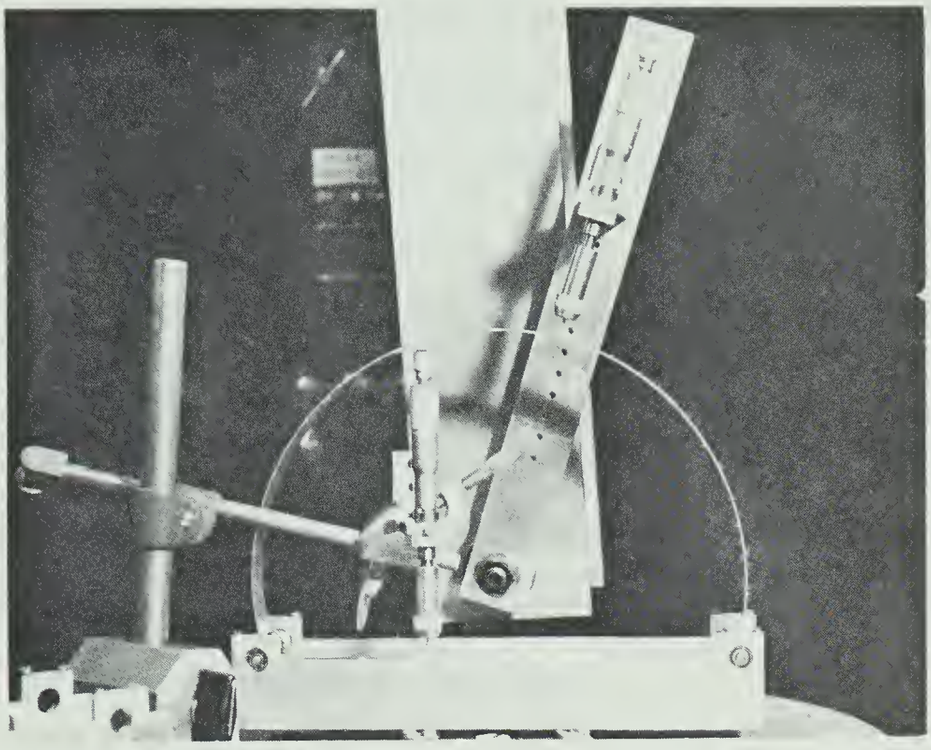

FIG. 3.1-1 MICROMETER PROBES

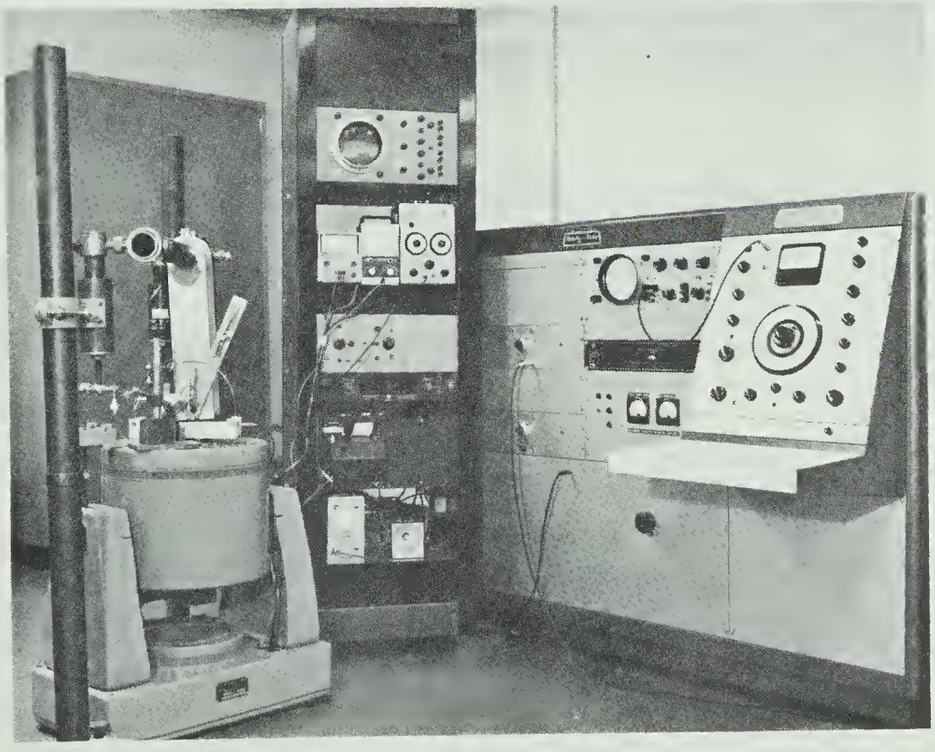

FIG. 3.1-2 GENERAL VIEW OF TESTING EQUIPMENT

The arches were rolled from strips cut from 6061-T6 aluminum sheets having a modulus of elasticity of 10^7 psi. The arches were bolted to one-half inch diameter steel shafts with bearing supports and in order to reduce the weight of the model, were mounted on a 3" x 1-1/2" x 1/4" aluminum channel. To reduce the effects of support flexure, the length of the supporting channel was chosen to be 11-inches.

To locate the points of zero displacement on the arch, a Chadwick-Helmuth Model No. 126A Stroboscope synchronized with the support displacement and equipped with a Chadwick-Helmuth Slip-Sync Model No. 105 AR Automatic Phase Shift was used.

3.2 Testing Procedure

Any arbitrary point on the arch has both radial and tangential displacements which are related by eq. 1.2-2. Because of this relationship, experimental evaluation of only one displacement was considered. Since radial displacements were easier to measure the theory is evaluated on this basis.

It was decided to use pinned-end supports for the experimental tests because previous experience with vibrating cantilever beams indicated that fixed-end conditions were difficult to attain [see Rae (24)].

To determine the accuracy of the micrometer measuring probe, a test was conducted comparing displacements as measured by the probe against those measured by a Gaertner Cathetometer which is an optical measuring device. The comparison is shown in Fig. 3.2-1. In view of the small difference, the micrometer probe was chosen as a reliable

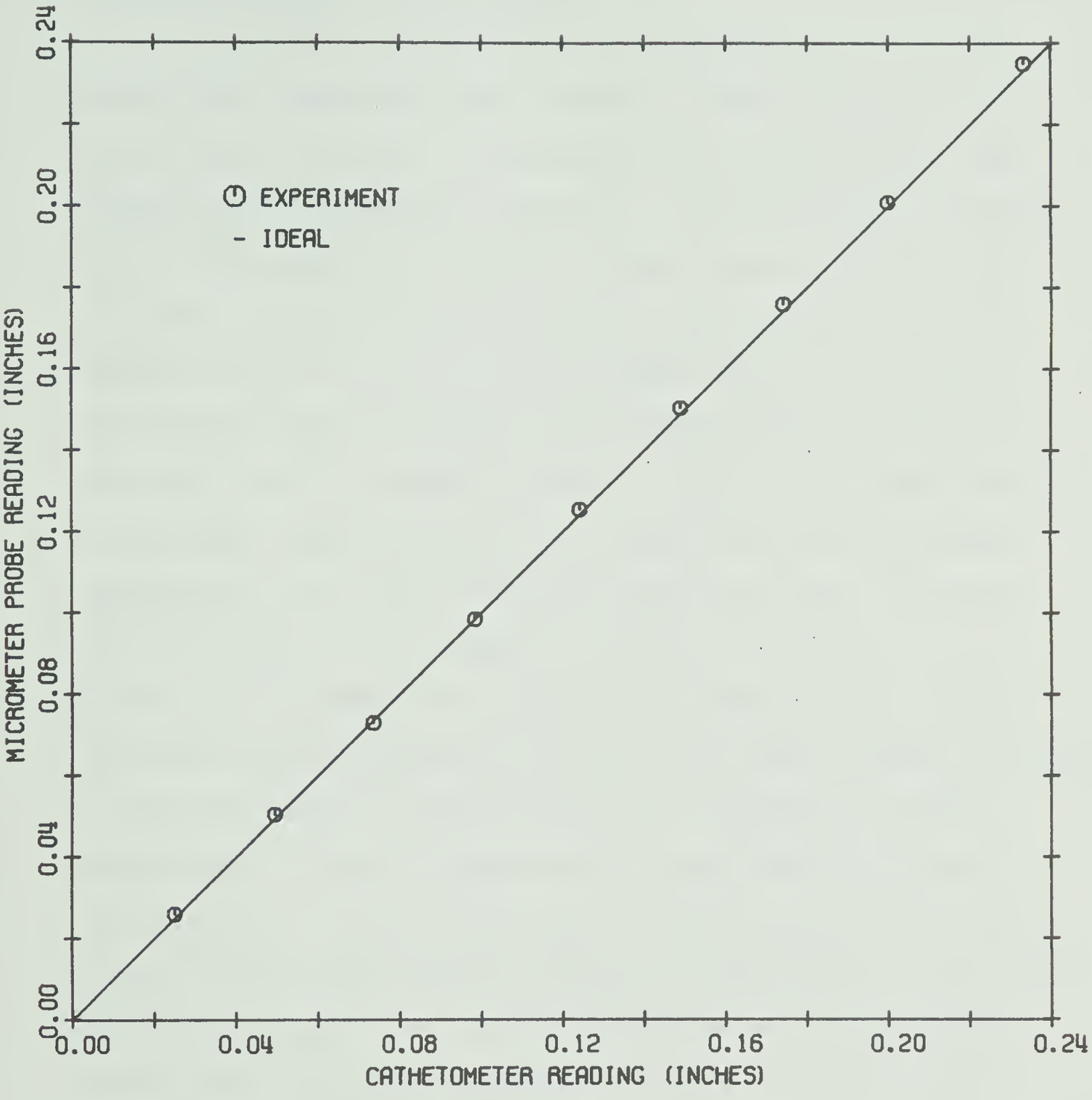

FIG. 3.2-1 COMPARISON OF DISPLACEMENT READINGS BETWEEN MICROMETER PROBE AND CATHETOMETER

means for measuring deflections. The precision of the probes was found to be approximately $\pm$ 0.005 inches.

In order to determine what arch parameters would yield the most reliable experimental data, a series of arches with various R/H and α values was tested. The arch behavior was observed under both symmetrical and unsymmetrical excitation. It was concluded that arches with $\alpha \approx 140$ degrees and $43 \leq R/H \leq 128$ were very susceptible to disturbances induced by the measuring probe. When arches with $\alpha < 90$ degrees and $R/H \approx 130$ were tested, they were very stiff and it was impossible to obtain a measurable displacement response at frequencies other than the first resonant frequency. Because of the force limitation of the shaker table and because of the resolution of the displacement measurement, it was found that the best operating range of the shaker table for these tests was between 5 and 125 H_z. On this basis, it was decided to build arches which had the first resonant frequency above $5H_z$ and at least the second below 125 H_z. With these frequency limitations, a forced response could then be obtained for frequencies up to the second mode, although for some arches a forced response was obtained for frequencies up to the fourth mode. To meet the above limitations, it was decided the best range of arches to test was $90° \leq \alpha \leq 125°$ which required the radius to be $5.01 \leq R \leq 6.00$ since the distance between supports was fixed at 10.02 inches for all tests. The condition of inextensibility i.e. $(R/k)^2 >> \lambda_n^2$ was satisfied if thicknesses of 0.032 and 0.042 inches and a width of one inch were used.

It was also observed that arches having large variations in

radius had experimental values considerably higher than those predicted by theory. Because of the higher experimental values, this would indicate that some unknown parameter is highly sensitive at this frequency and is exciting the arch amplitude beyond the theoretical value. The best circular arches were obtained by using a Di-Arco, No. 2A precision three-roll roller. The arches were checked by tracing the arch outline on paper and then drawing in the best-fit radius. Measurements were taken and a radius, $R \pm \frac{1}{2} H$, was assigned. The theoretical solutions were based on the radius ($R \pm \frac{1}{2} H$) which most closely matched the theoretical and experimental values of the resonant frequency for the first four modes. Any arch having a radius variation greater than one-half the thickness was rejected. The values of α for the arches were calculated on the basis of the best-fit radius and by using the distance between the arch supports of 10.02 inches.

As noted in Chapter II, under the assumptions used in the development of the theory, some damping is present in the system, however, it was assumed to be small and was neglected in the theoretical analysis. To reduce the effects of damping in the experimental tests, arches were excited at frequencies sufficiently far from resonant conditions since the effect of damping is most pronounced at resonant conditions. To meet this condition, it was decided to excite arches at frequencies such that the maximum magnificiation ratio (U/G) was kept below the value of four.

To check the effects of damping in the system, one LVDT (linear variable differential transformer) probe was attached to the crown of the arch and another LVDT probe was attached to the support.

Under symmetrical excitation (to ensure no tangential displacement at the crown) a simultaneous trace of the output from the two LVDT's was recorded, using a Brush Oscillograph Model No. 13-5335-00, at various frequencies. As shown in Fig. 3.2-2, the two outputs are nearly in-phase or 180 degrees out-of-phase. On the basis of these phase angles, it was concluded that damping was small and could be omitted from the theoretical analysis. Although a frequency trace was obtained only for one point on the arch, other points were assumed to behave similarly.

By comparing displacements obtained from taking readings on the outside and inside circumference of the arch, a check was made on the zero shift of the static position of the arch. Since the differences in the readings were in the range of the precision of the micrometer probe, it was decided that sufficiently reliable results would be obtained by taking readings on the outside circumference only.

Since the arch vibrated about its static position, the amplitudes of the radial displacements were obtained by taking the difference in the readings between the dynamic and static reading. For example, consider an arbitrary point P, shown by the static position A in Fig. 3.2-3, for which a reading was taken. Point P is moving continuously and reaches its maximum displacement when P is at P' in position B, for which a dynamic reading was taken. The difference in the two readings is U_A, where U_A represents the absolute radial displacement. In order to eliminate the error ε which would occur if both the static and dynamic readings were taken with the probe at the same

$\Omega < \omega_2$ (Ω = 19.3 H_z)

$\omega_2 < \Omega < \omega_4$ (Ω = 60.4 H_z)

$\Omega > \omega_4$ (Ω = 160.0 H_z)

FIG. 3.2-2 DISPLACEMENT TRACES FOR ARCH AND SUPPORT

R/H = 133.3 and α = 116.5 DEGREES

angular position, it was necessary to move the probe to position P' when taking the dynamic reading. Generally, the tangential displacement for P was less than 0.15 inches, giving a maximum angular difference in the two positions of less than two degrees for an arch with a five-inch radius. Experimental data was taken at two-inch intervals along the outside circumference.

For each frequency a series of four readings, each with a different support displacement, was taken for each position on the arch. The support displacements were divided into four equally spaced increments between the two extremes used for the particular test. An average value of absolute arch displacement divided by the support displacement (i.e. U_A/G) was calculated from the four readings for each position.

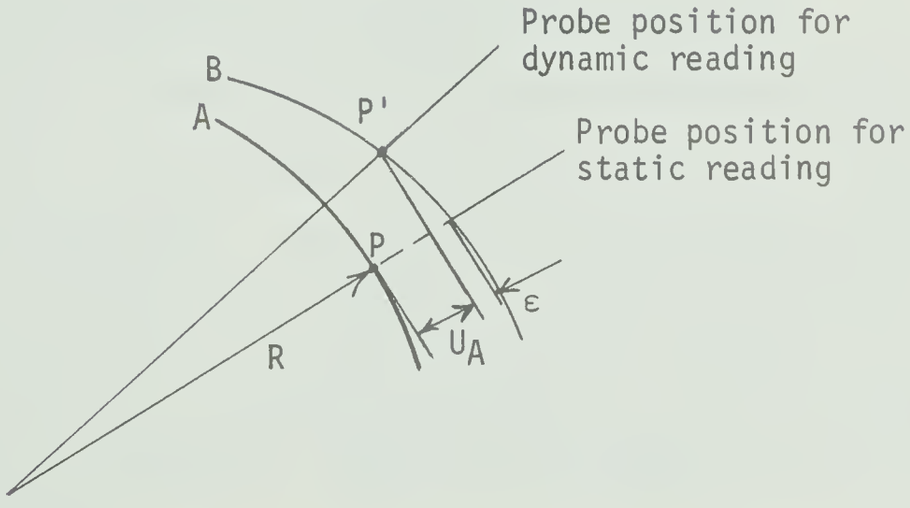

FIG. 3.2-3 POSITION OF MICROMETER PROBE DURING TEST

When arches were excited near a resonant frequency, it was observed that the amplitude of the arch displacement was highly sensitive to slight variations in the forcing frequency. (This is another indication that damping was small.) If $U_A/G < 4$, the forcing frequency would be sufficiently removed from the resonant frequency yet be close enough to the resonant mode ensuring a measurable arch amplitude. Generally, the maximum value of U_A/G was kept between one and two. It was also observed for some arches excited beyond the fourth resonant frequency, out-of-plane modes were excited. These out-of-plane vibrations occurred at frequencies approximately sixteen times the frequency of the first flexural mode which agrees with the observations made by Volterra and Morell (15). These out-of-plane vibrations are excited because of the difficulty in aligning the plane of displacement with the plane of the arch.

3.3 Presentation of Theoretical and Experimental Results

Results are presented for four arches with R/H values of 121.2, 133.3, 157.8 and 179.4 and α values of 100.2, 116.5, 97.2 and 119.2 degrees respectively. For each arch, the first four mode shapes are presented, followed by the results for symmetrical excitation, and then by the results for unsymmetrical excitation. For both symmetrical and unsymmetrical excitations, results are presented for four different forcing frequencies.

Since damping was small, the experimental resonant frequencies were determined by adjusting the forcing frequency until maximum de-

flections occurred in the arch. This frequency could be obtained within $\pm$ 0.3 H_z. To obtain the mode shapes of free vibration, the arch amplitudes were measured as the arch vibrated at the resonant frequency. Figure 3.3-1 shows a photographic view of the first four modes for various positions of the arch as it moved through its cycle. At resonant conditions, a support displacement of less than 0.005 inches was sufficient to have arch amplitudes in the order of 0.2 inches giving a magnification factor with values greater than 40. Since it was possible to obtain large magnification ratios at resonant frequencies, this indicated that at a resonant frequency, the arch was essentially under the condition of free vibration. Hence, under these conditions, sufficiently accurate mode shapes could be measured. For the unsymmetrical modes, the experimental data was normalized such that the largest experimental displacement coincided with the displacement on the theoretical curve for the same point. For the symmetrical modes, the experimental data was normalized with respect to the point at $\phi = 0$.

The theoretical solution as given by eq. 2.5-8 for symmetrical excitation and by eq. 2.6-12 for unsymmetrical excitation yields the radial displacement due to arch deformation only, i.e. the effect of support movement on the arch displacement is not considered. The experimental values are absolute displacements which requires a modification of the theoretical solution to account for the support movement before a comparison between theory and experiment can be made. The modified theoretical solution is

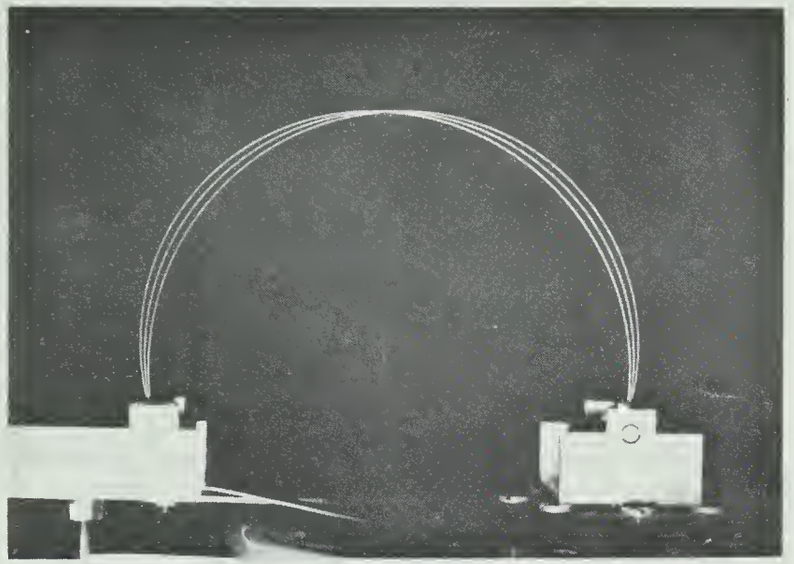

First Mode

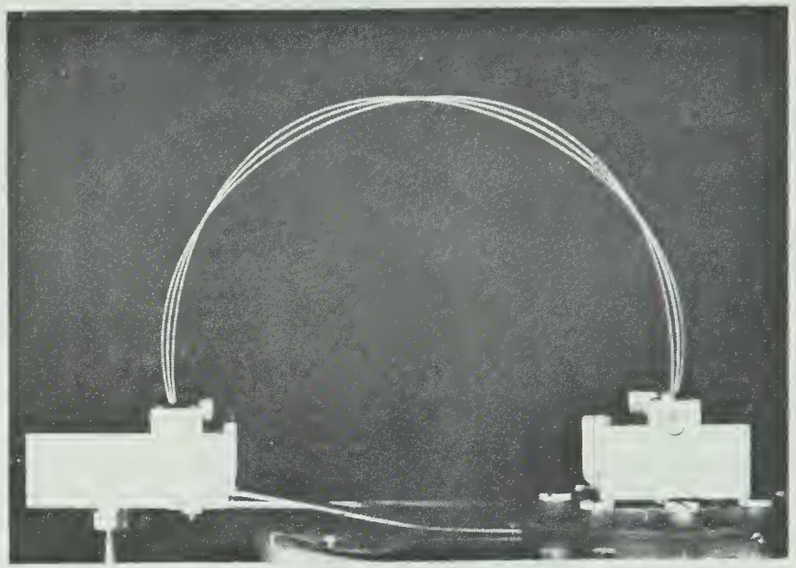

Third Mode

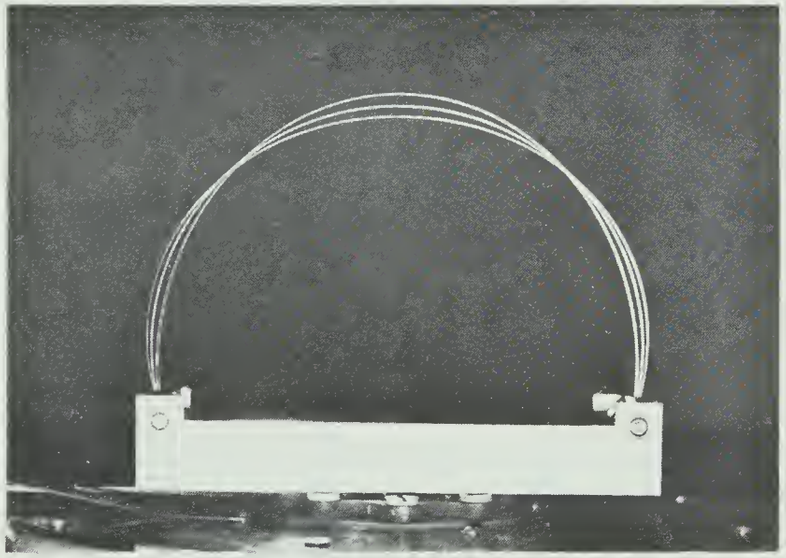

Second Mode

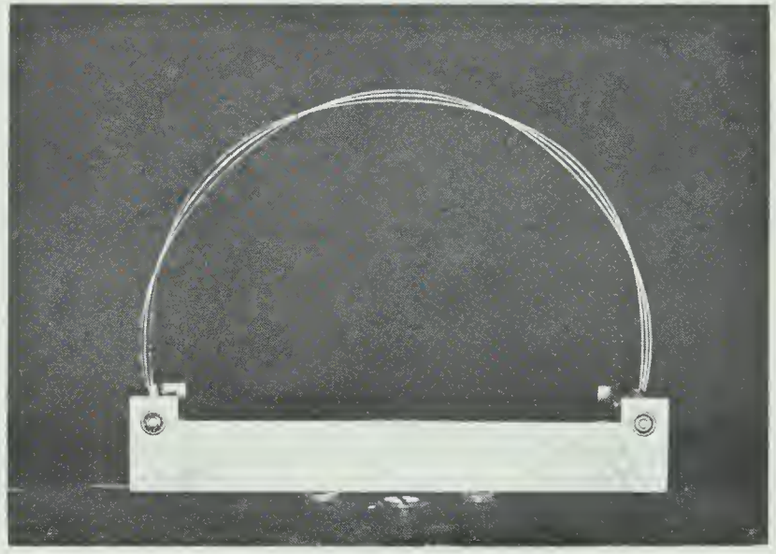

Fourth Mode

FIG. 3.3-1 FIRST FOUR FREE MODES; R/H = 163.4 AND α = 106.7 DEGREES

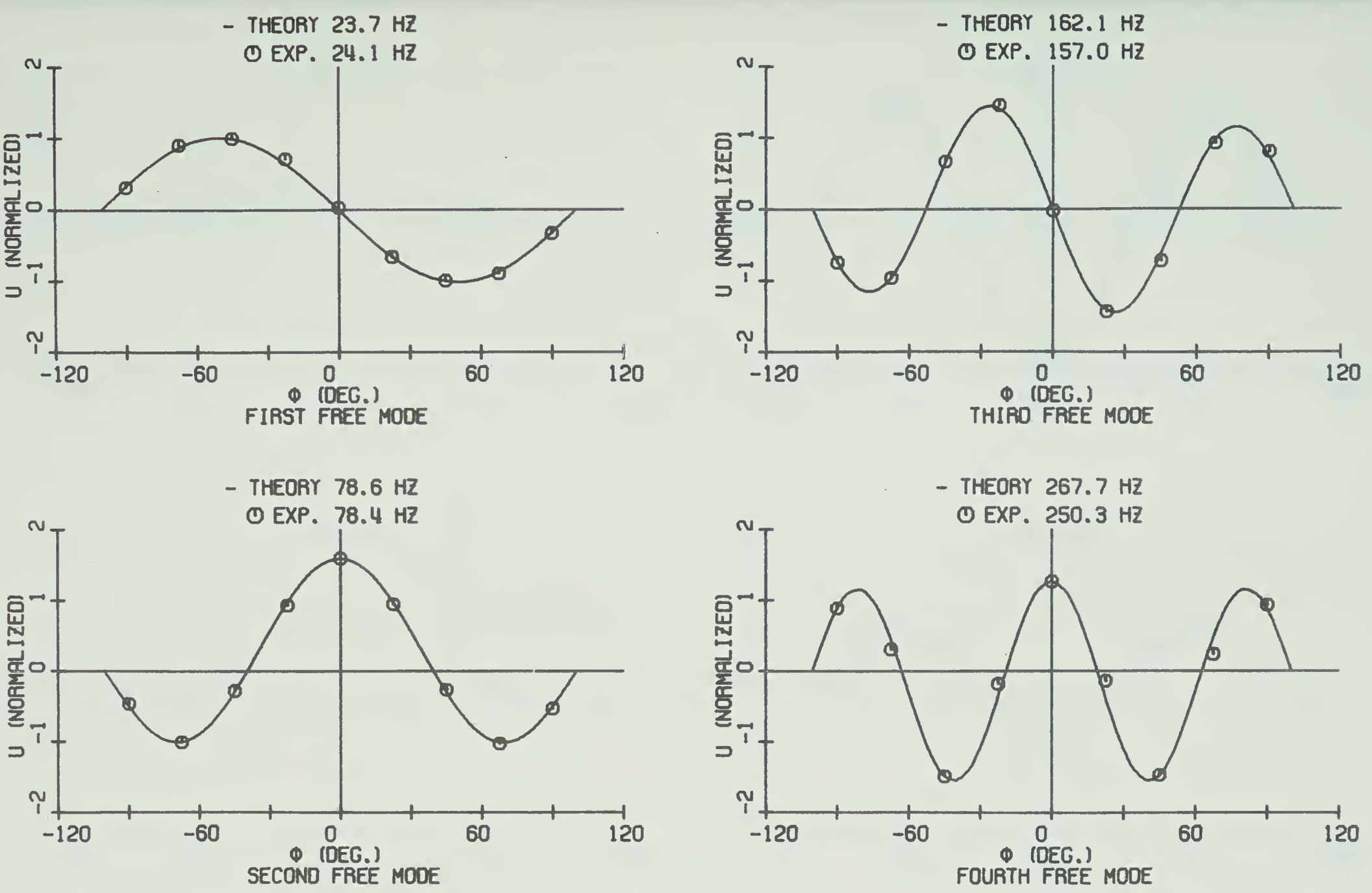

α = 100.2 DEG. R = 5.09 IN. H = 0.042 IN.

FIG. 3.3-2 NORMALIZED RADIAL DISPLACEMENT, R/H=121.2

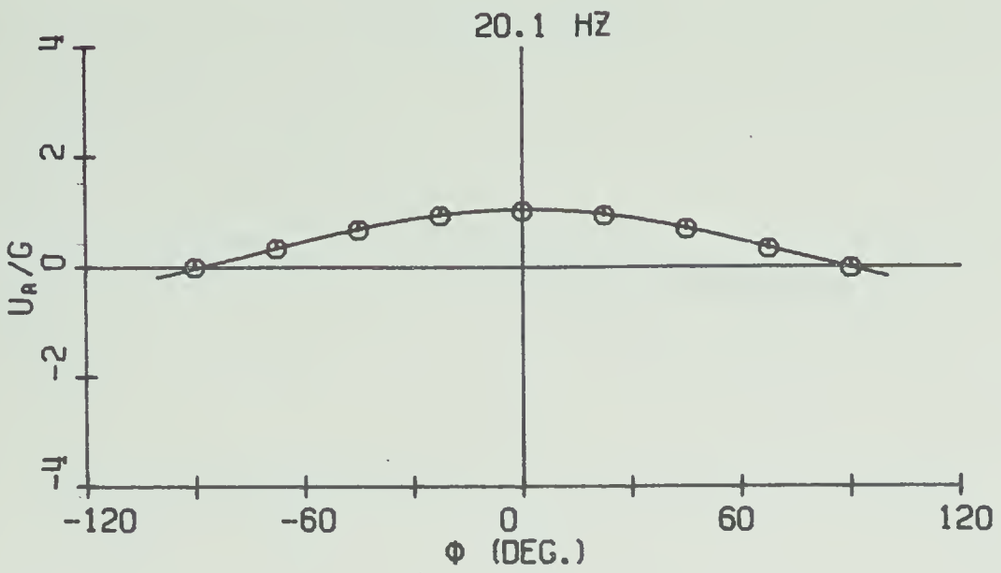

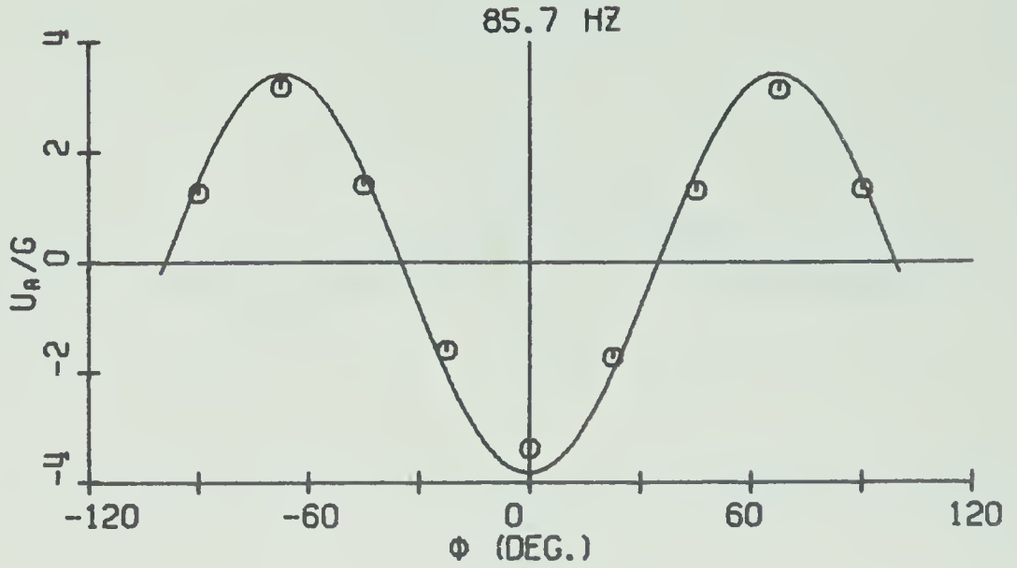

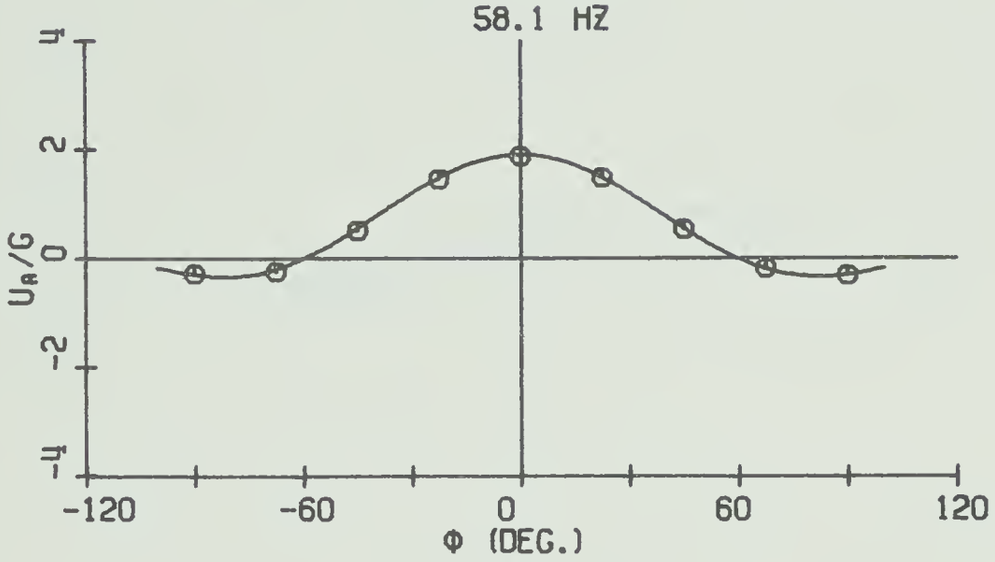

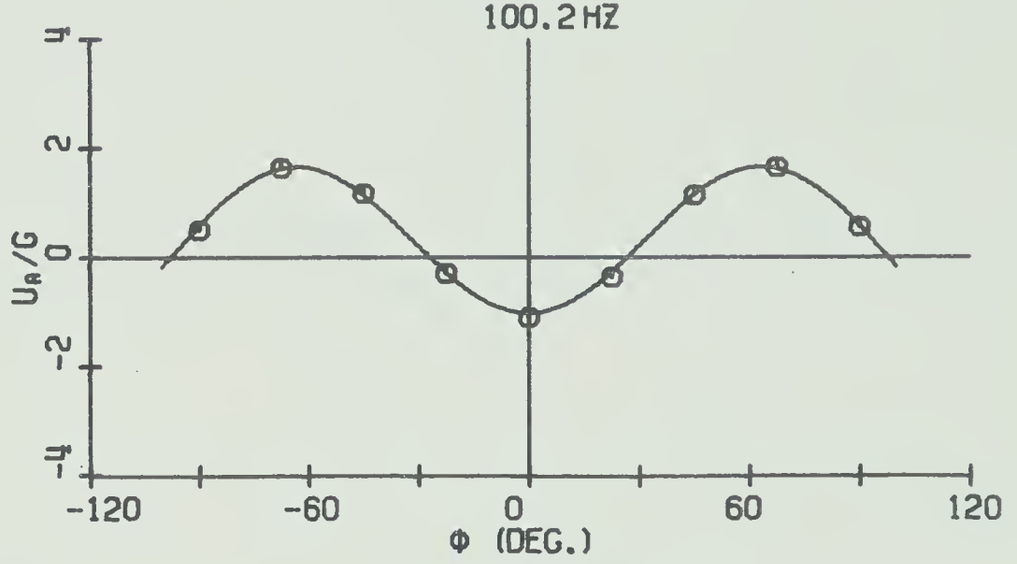

α = 100.2 DEG. H = 0.042 IN.

R = 5.09 IN.

Ⓘ EXPERIMENT

– THEORY

FIG. 3.3-3 MAGNIFICATION RATIO; SYMMETRICALLY FORCED, R/H=121.2

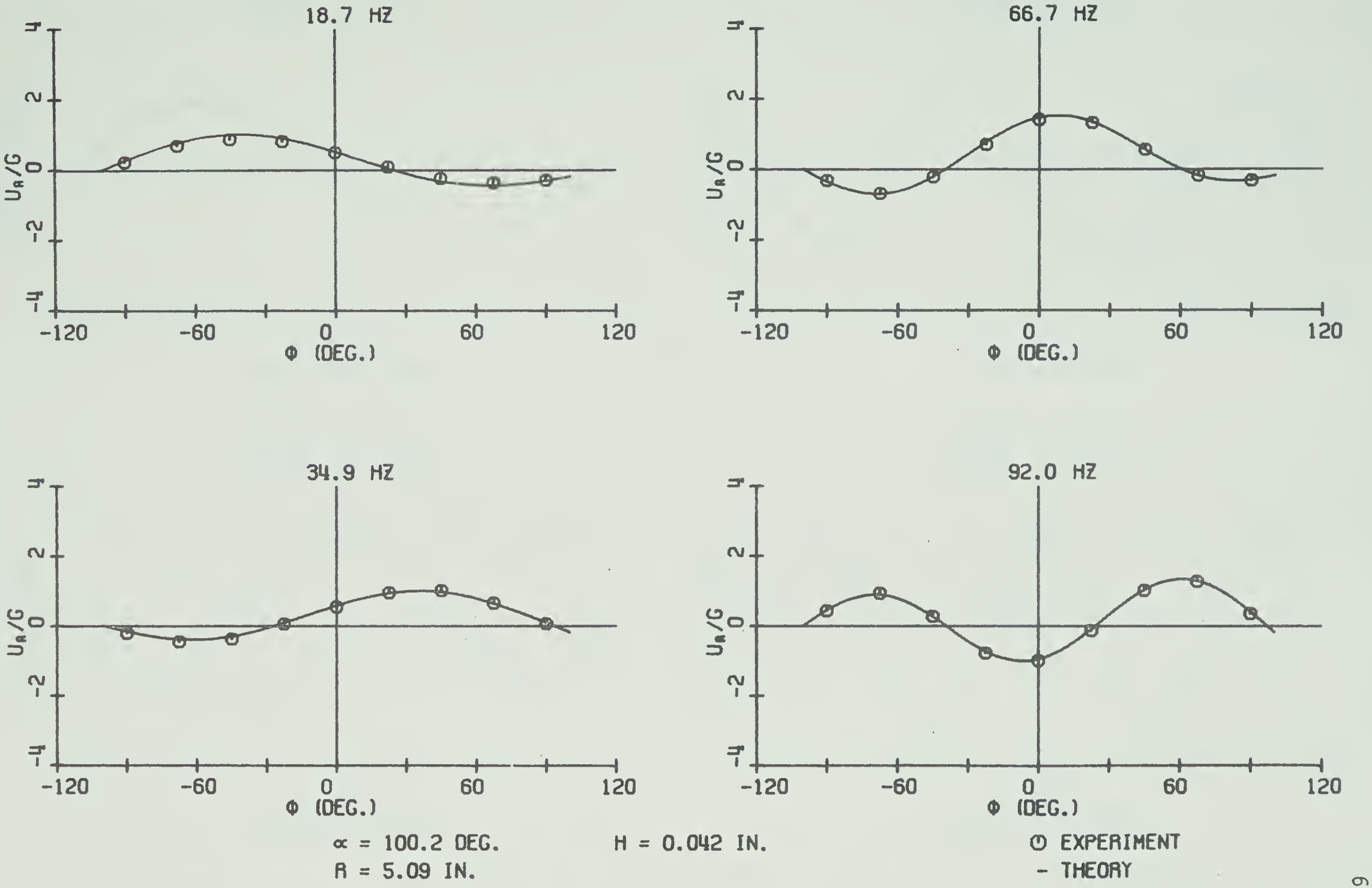

FIG. 3.3-4 MAGNIFICATION RATIO; UNSYMMETRICALLY FORCED, R/H=121.2

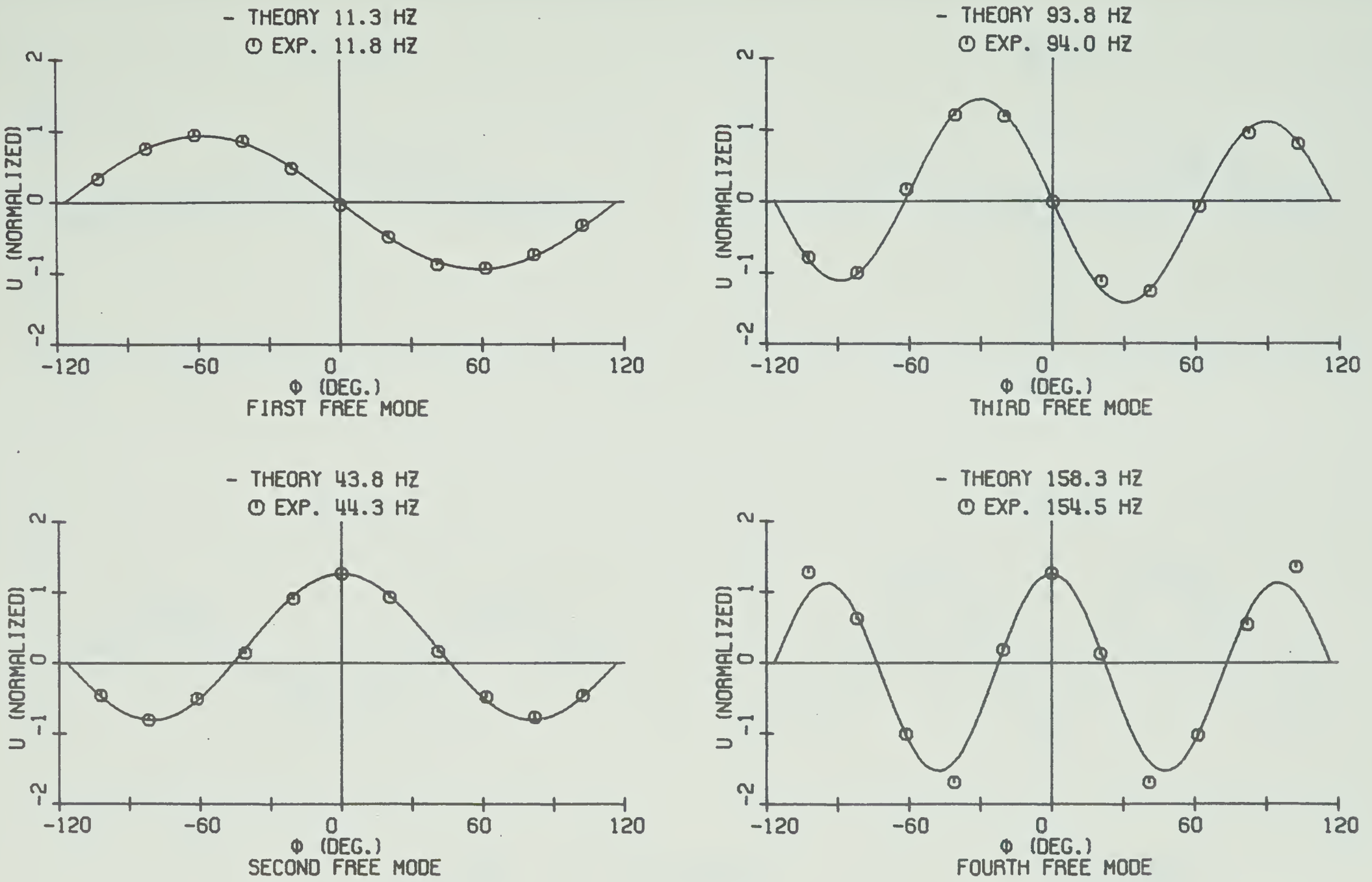

α = 116.5 DEG. R = 5.60 IN. H = 0.042 IN.

FIG. 3.3-5 NORMALIZED RADIAL DISPLACEMENT, R/H=133.3

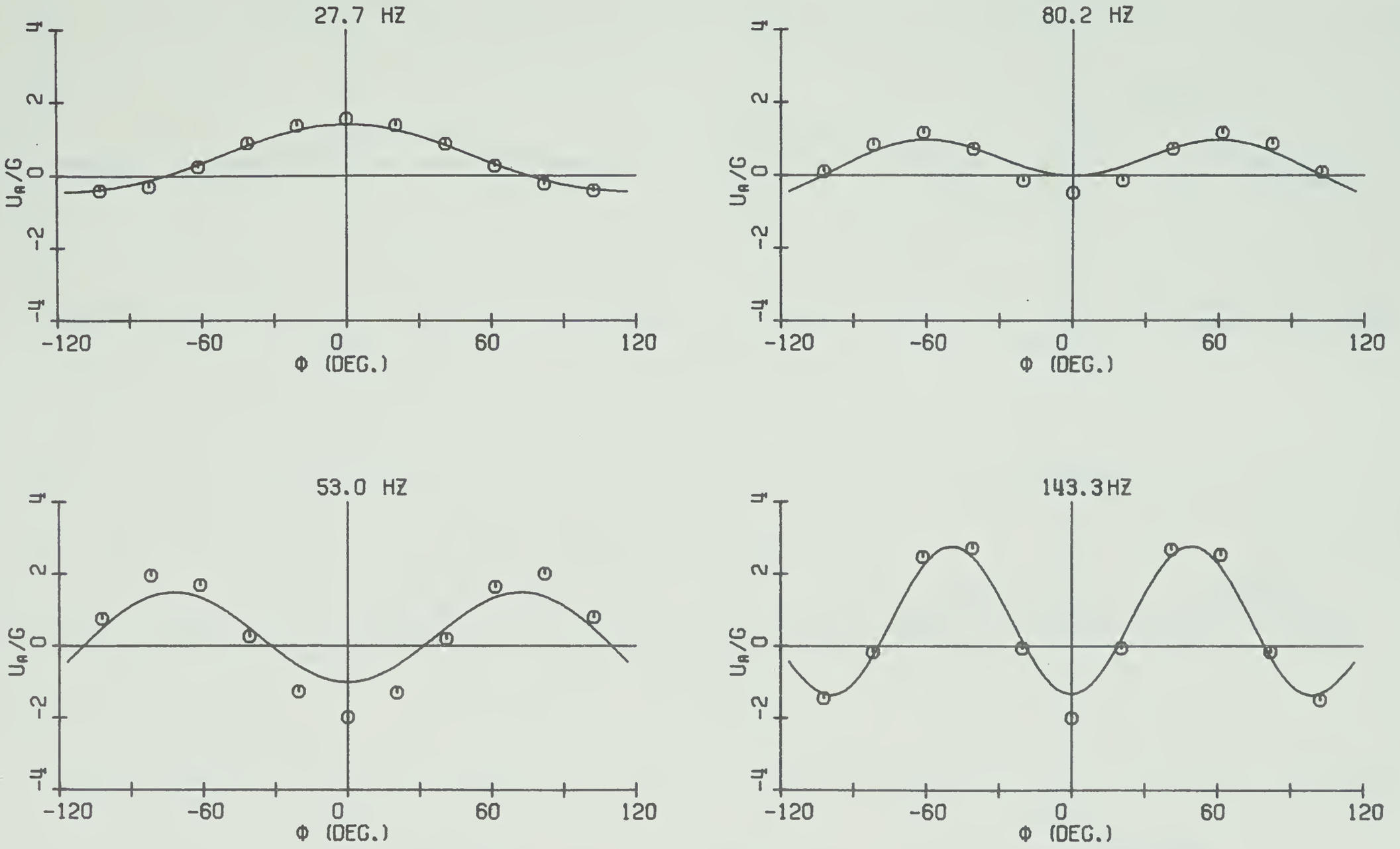

FIG. 3.3-6 MAGNIFICATION RATIO; SYMMETRICALLY FORCED, R/H=133.3

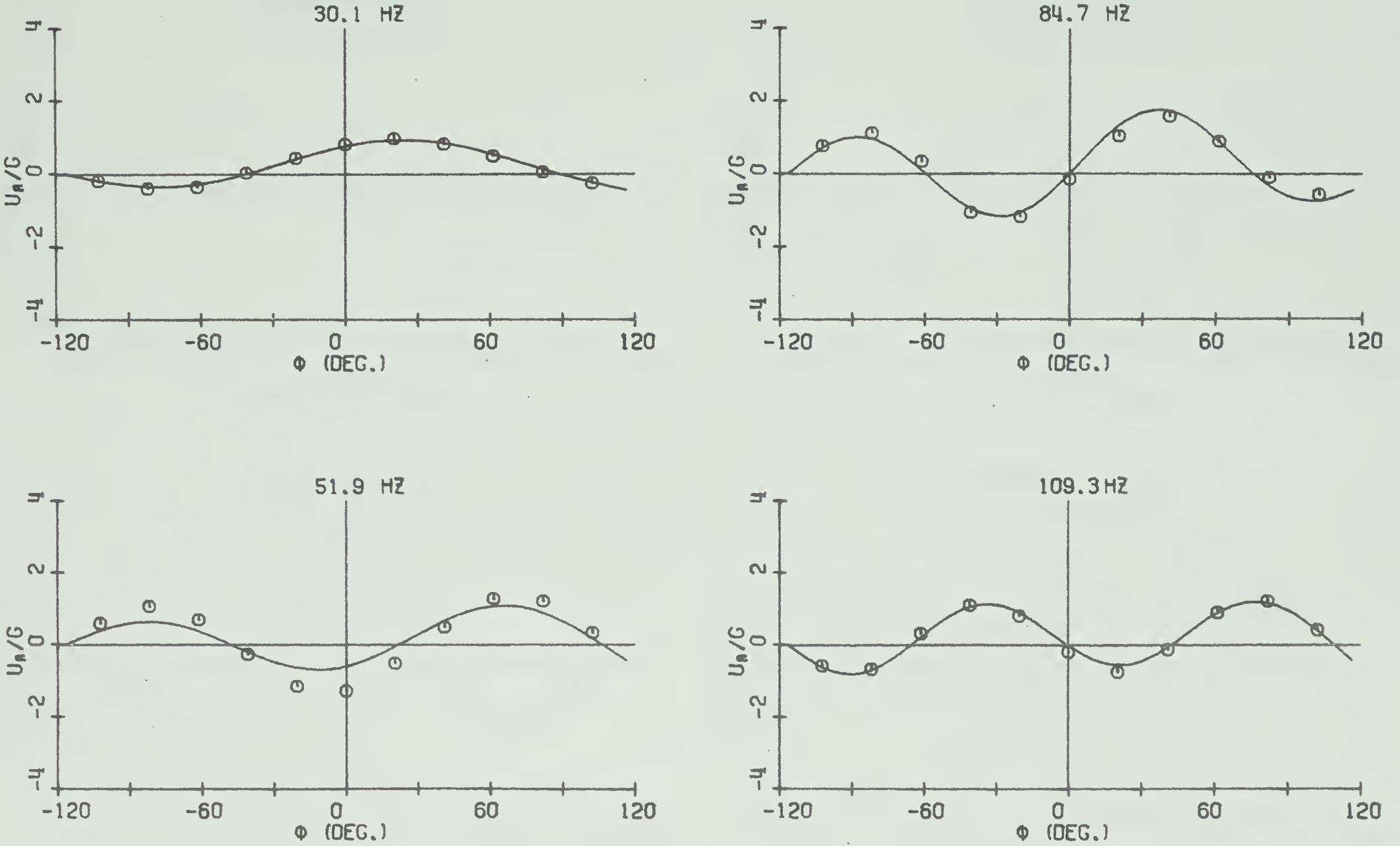

FIG. 3.3-7 MAGNIFICATION RATIO; UNSYMMETRICALLY FORCED, R/H=133.3

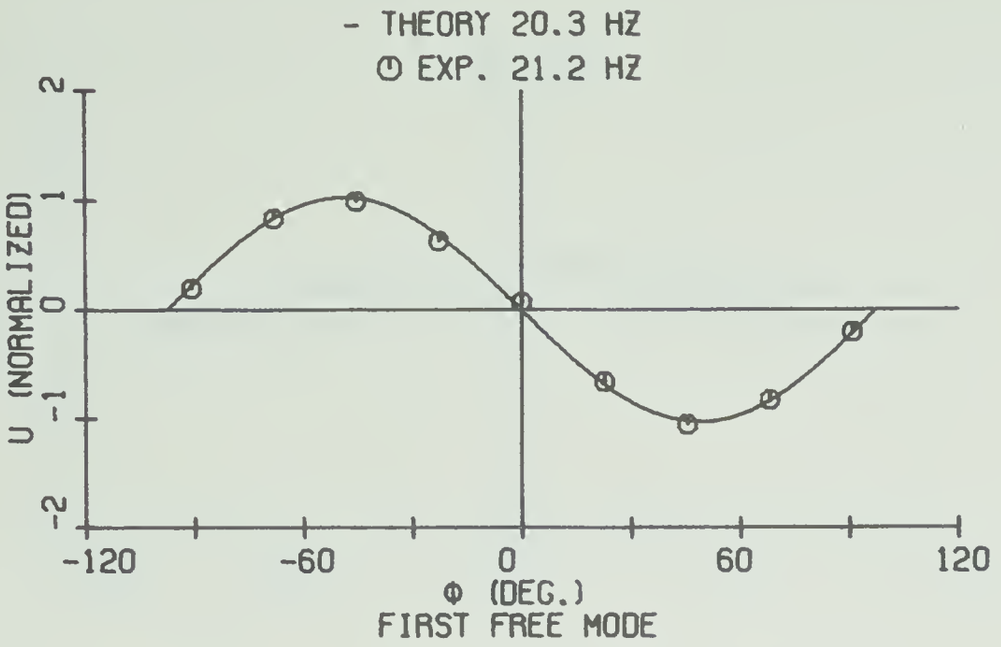

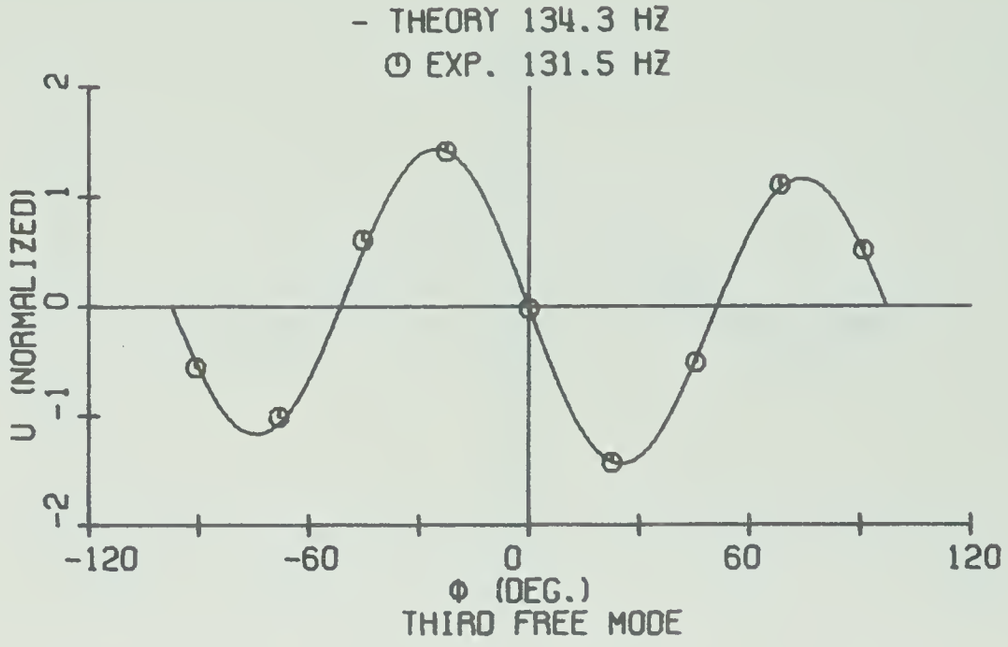

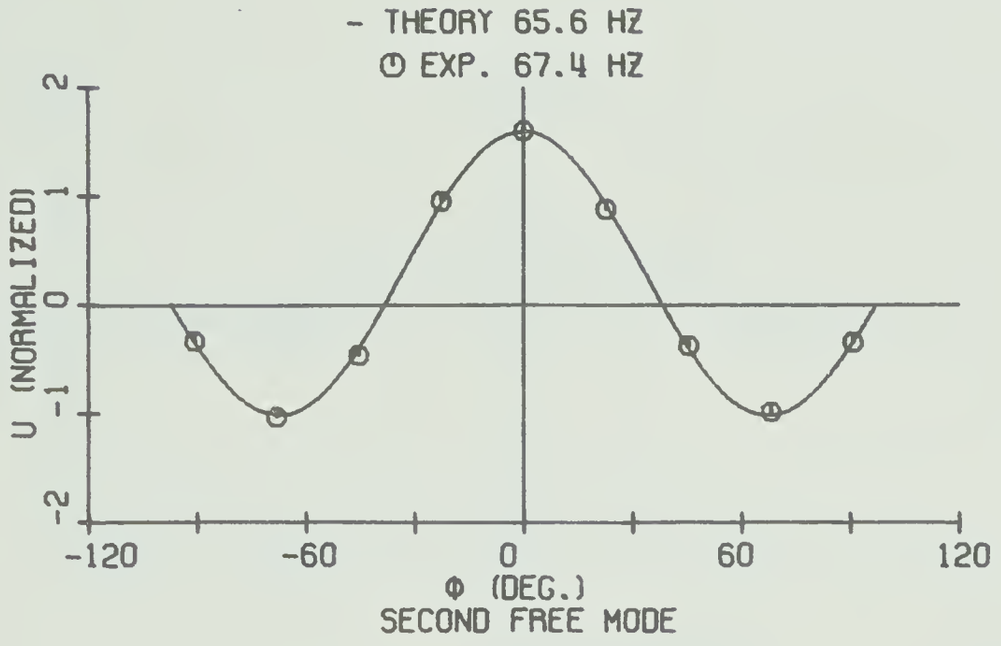

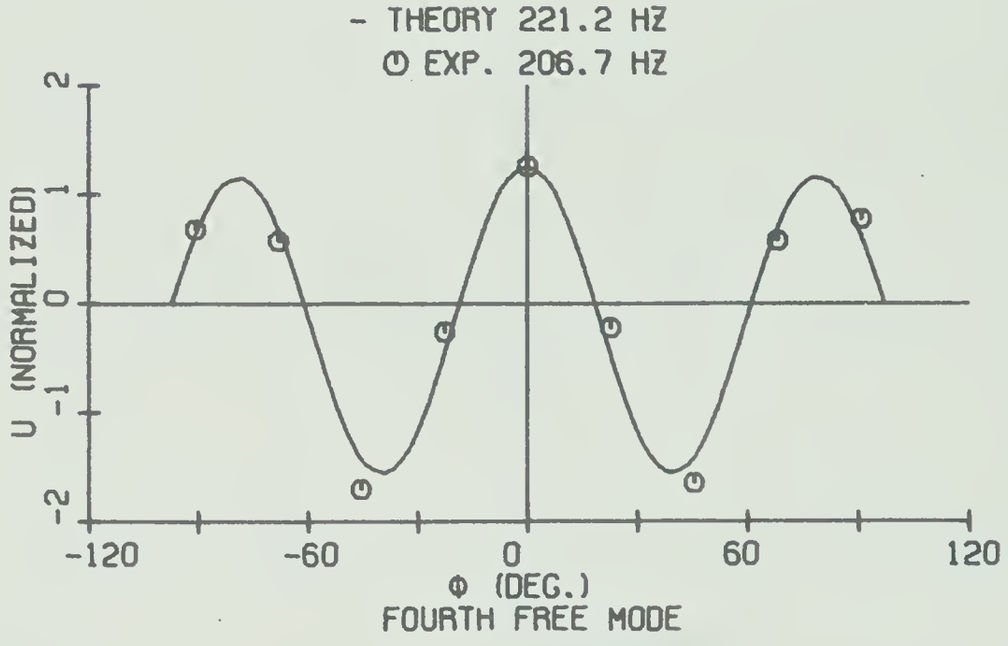

α = 97.2 DEG. R = 5.05 IN. H = 0.032 IN.

FIG. 3.3-8 NORMALIZED RADIAL DISPLACEMENT, R/H=157.8

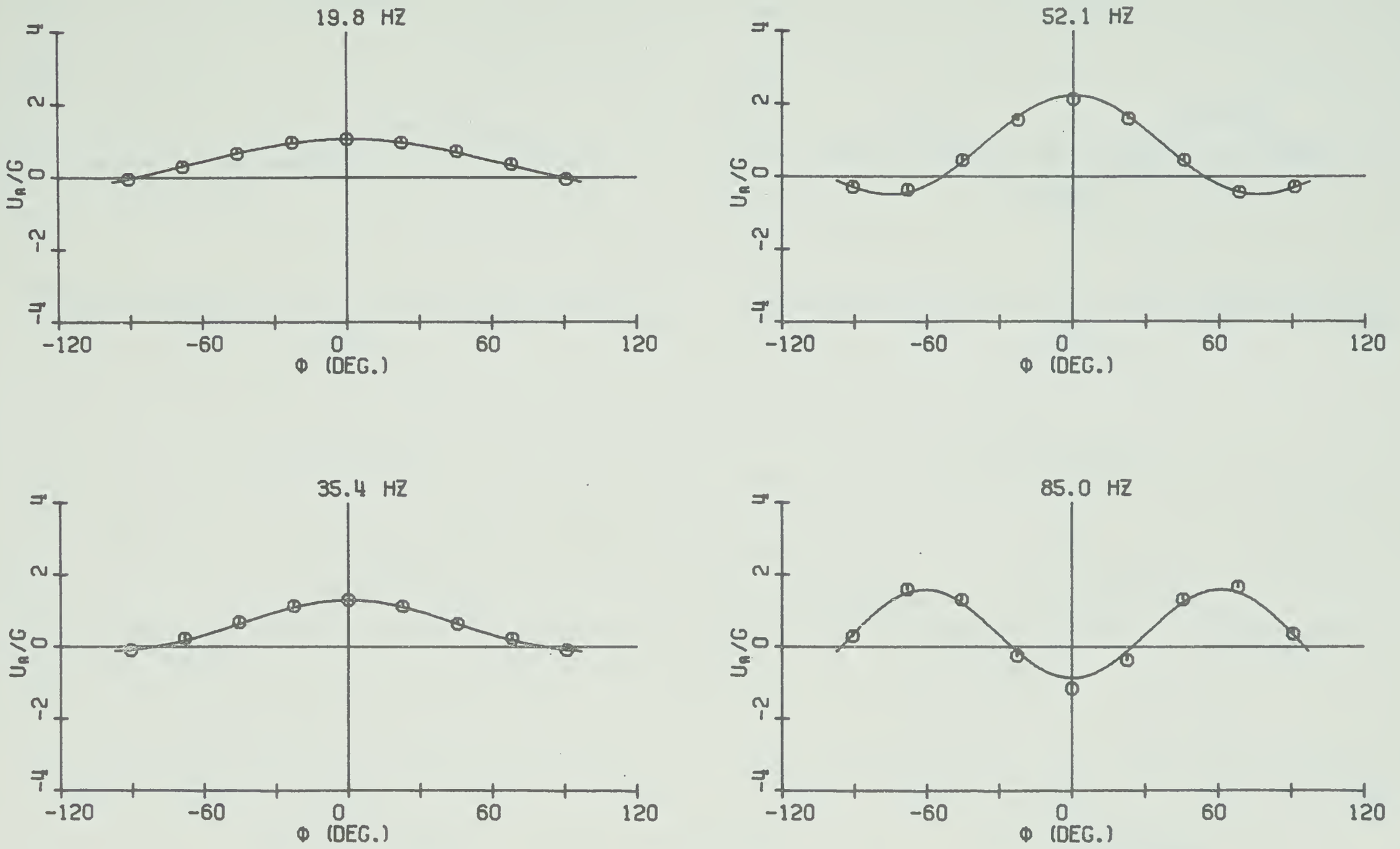

α = 97.2 DEG.
R = 5.05 IN.

H = 0.032 IN.

⊙ EXPERIMENT
– THEORY

FIG. 3.3-9 MAGNIFICATION RATIO; SYMMETRICALLY FORCED, R/H=157.8

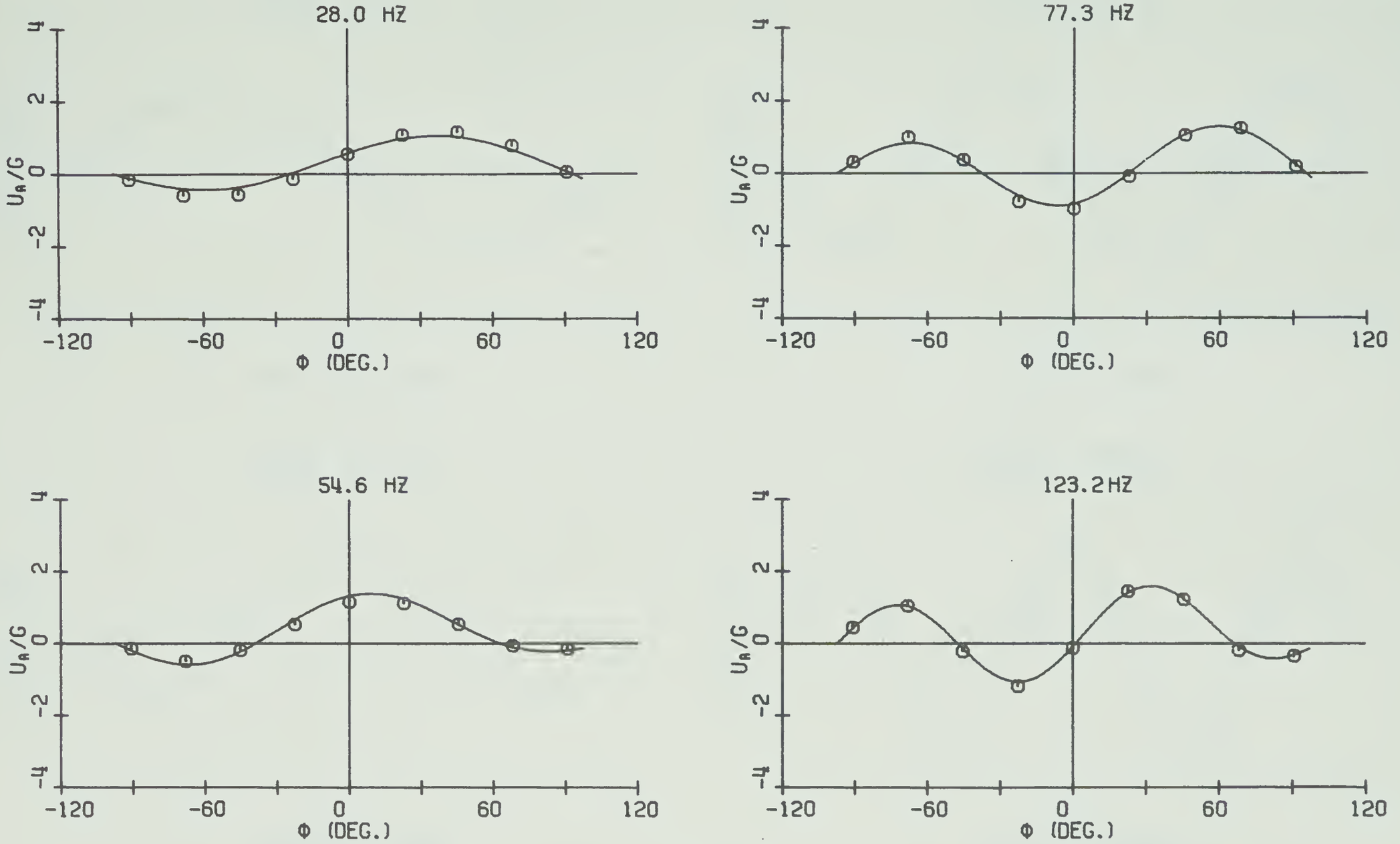

α = 97.2 DEG.
R = 5.05 IN.

H = 0.032 IN.

⏀ EXPERIMENT
– THEORY

FIG. 3.3-10 MAGNIFICATION RATIO; UNSYMMETRICALLY FORCED, R/H=157.8

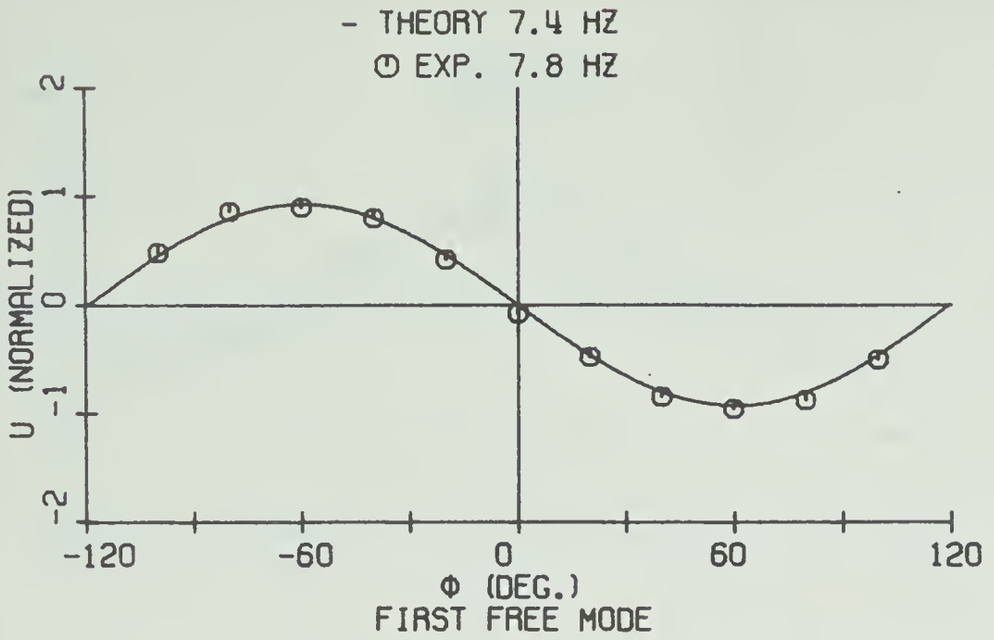

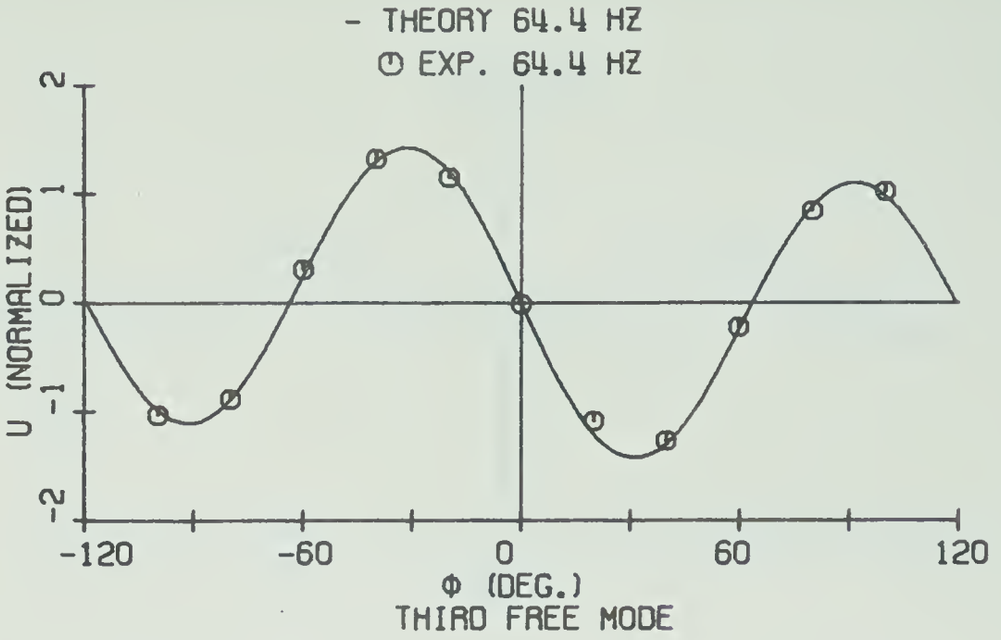

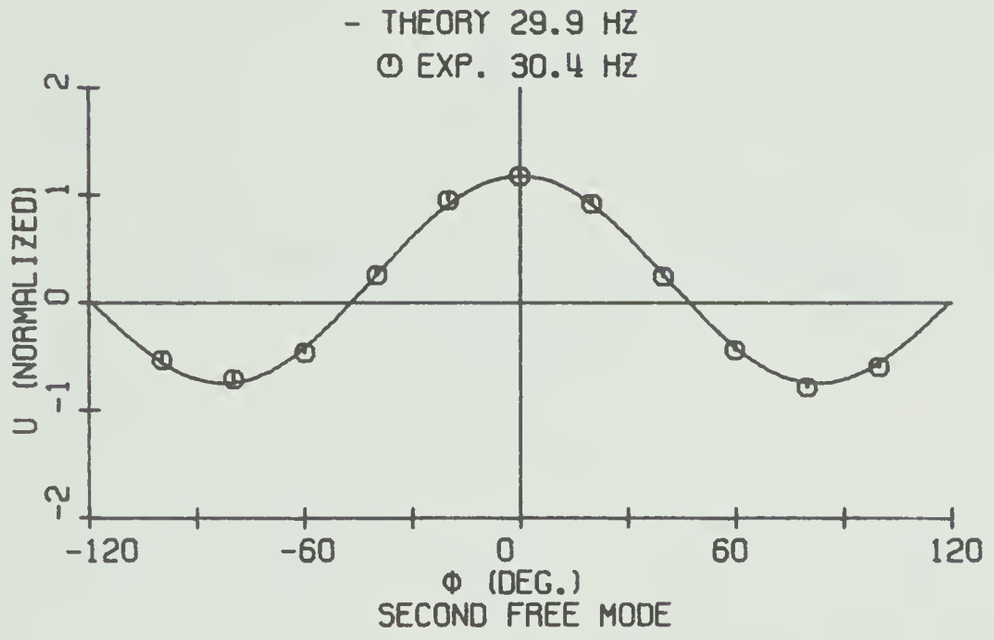

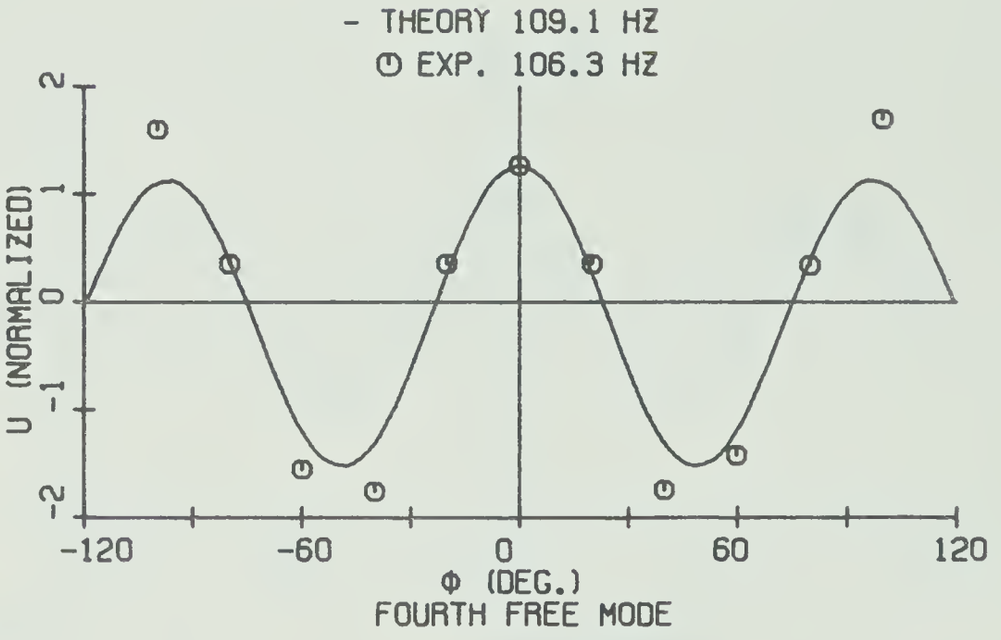

α = 119.2 DEG. R = 5.74 IN. H = 0.032 IN.

FIG. 3.3-11 NORMALIZED RADIAL DISPLACEMENT, R/H=179.4

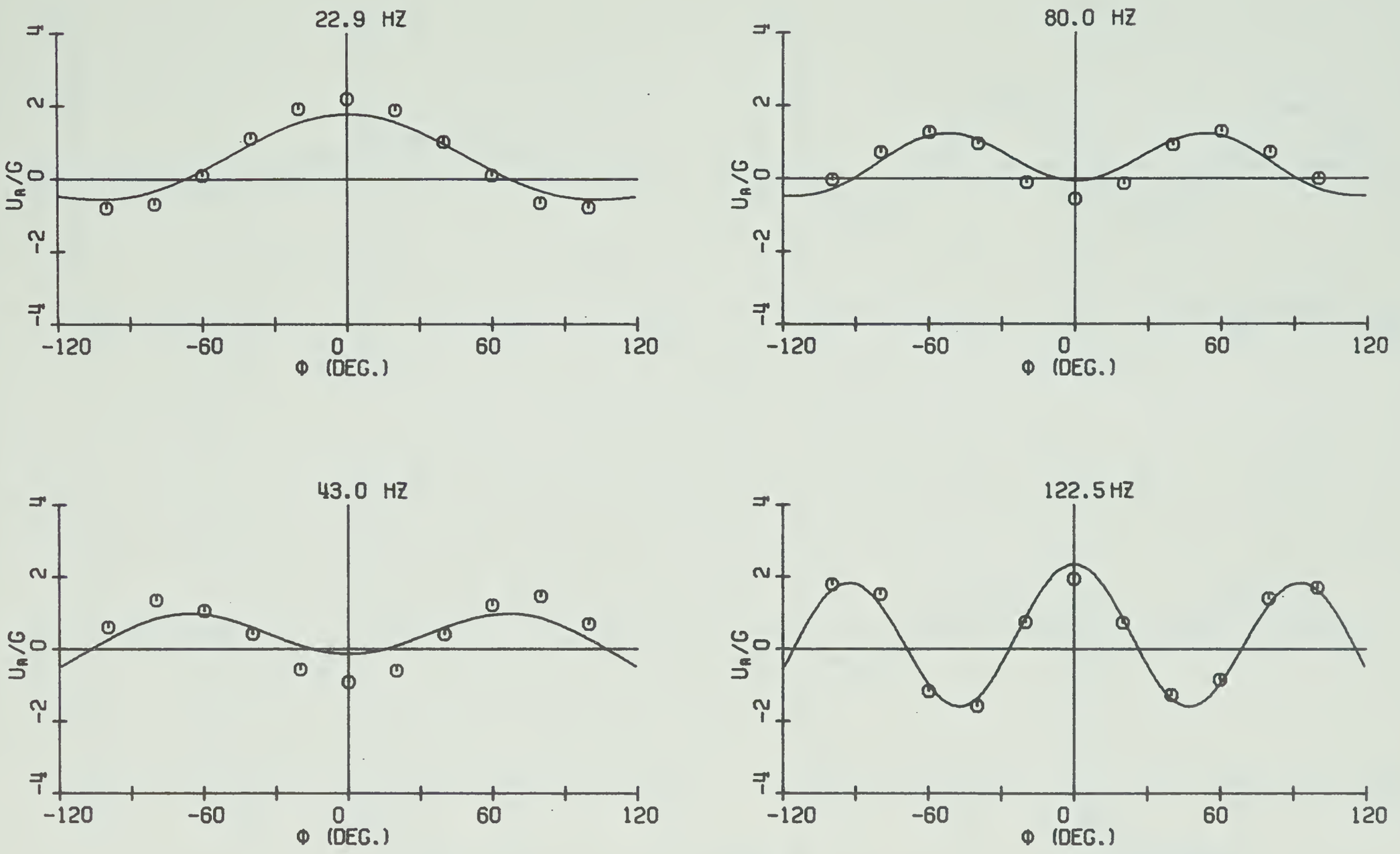

FIG. 3.3-12 MAGNIFICATION RATIO; SYMMETRICALLY FORCED, R/H=179.4

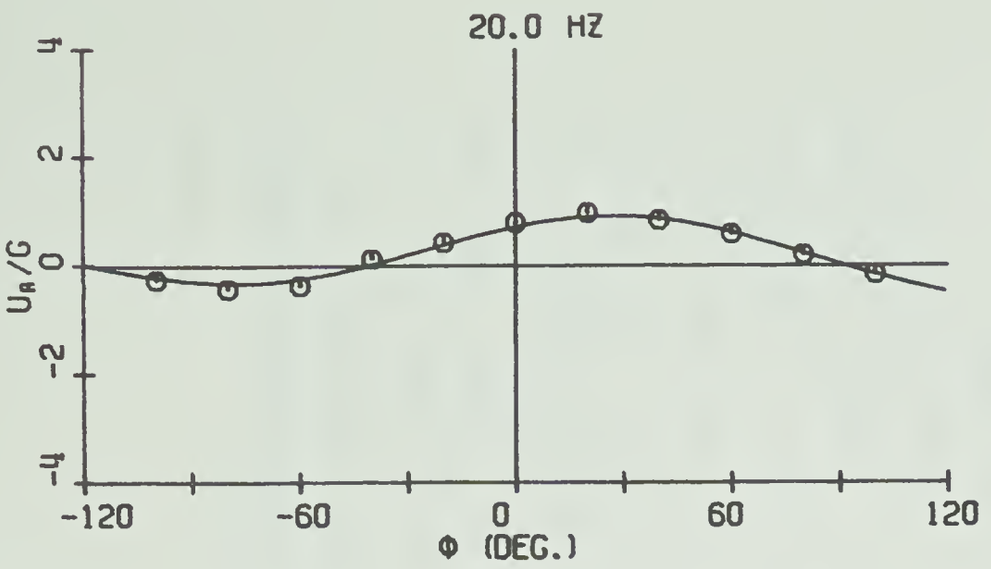

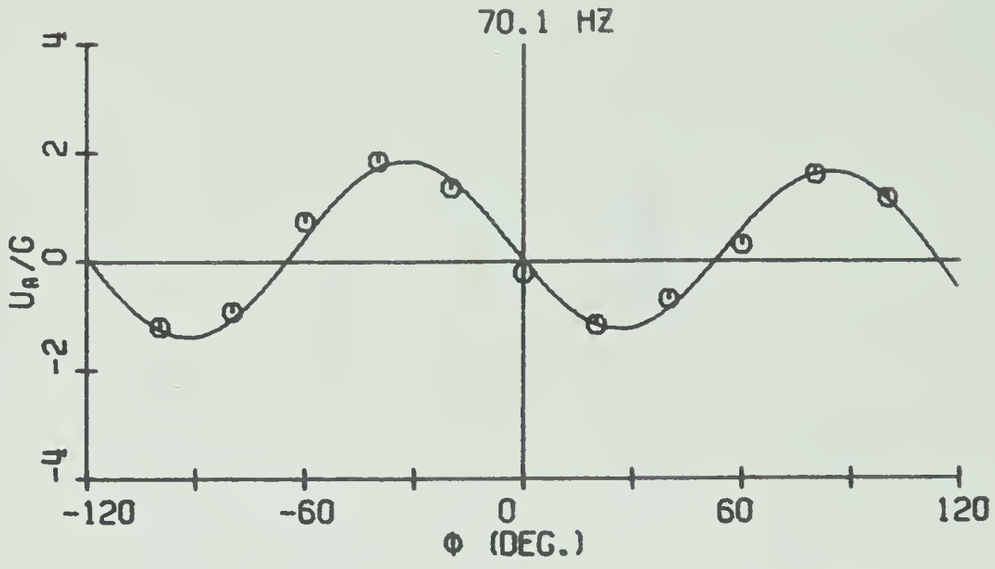

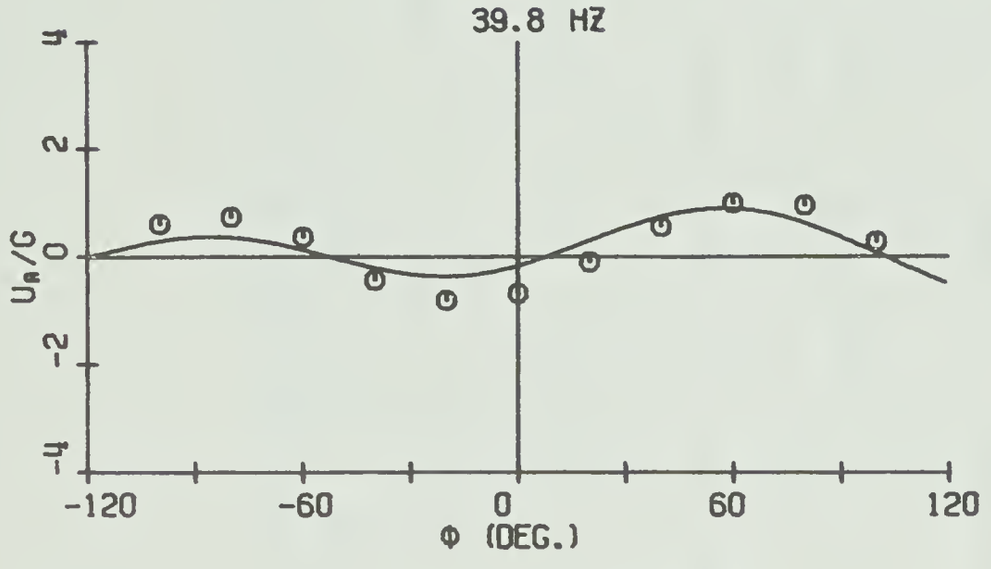

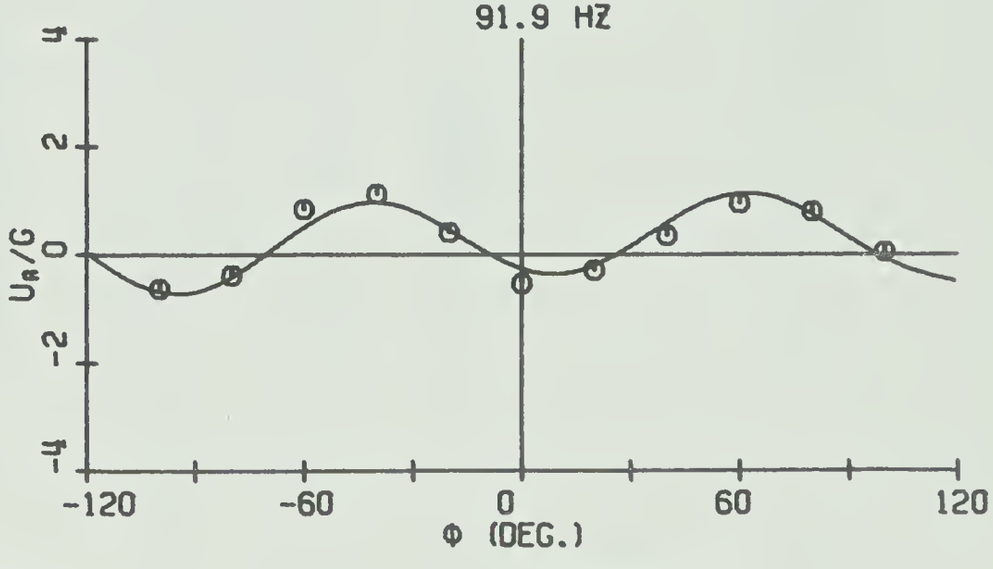

α = 119.2 DEG.
R = 5.74 IN.

H = 0.032 IN.

⊙ EXPERIMENT
– THEORY

FIG. 3.3-13 MAGNIFICATION RATIO; UNSYMMETRICALLY FORCED, R/H=179.4

$$\frac{U_A}{G} = \left[\sum_{j=1}^{\infty} \frac{\Omega^2 D_j' U_j(\phi)}{\omega_j^2 - \Omega^2} + \cos\phi\right] \sin \Omega t \qquad 3.3\text{-}1$$

for symmetrical excitation, and

$$\frac{U_A}{G} = \left[\sum_{j=1}^{\infty} \frac{\Omega^2 D_j' U_j(\phi)}{\omega_j^2 - \Omega^2} + \frac{\sin(\phi+\alpha)}{2\sin\alpha}\right] \sin \Omega t \qquad 3.3\text{-}2$$

for unsymmetrical excitation, where U_A denotes absolute radial displacement and G is the amplitude of support displacement.

A comparison between theory and experiment for the mode shapes and forced excitations is shown in Fig. 3.3-2 through to 3.3-13.

3.4 Discussion of Theoretical and Experimental Results

A summary is given in Table 3.4-1 comparing the theoretical and experimental values for the resonant frequencies together with the percentage difference. It can be seen that good agreement was obtained. The experimental values of the resonant frequencies are generally higher than the theoretical ones for modes one and two and lower for modes three and four. A possible cause for this is friction acting at the bearing supports forcing the experimental values to be higher at the lower modes. However, at the higher modes, it is possible that the inertia of the support shafts overcomes the frictional effects resulting in lower experimental values than those predicted by theory. Good agreement between theory and experiment for all mode shapes was obtained.

Arch \ Mode	*	1	2	3	4
$\frac{R}{H}$ = 121.2	T	23.7	78.6	162.1	267.7
	E	24.1	78.4	157.0	250.3
	D	+ 1.7	- 0.3	- 3.1	- 6.5
$\frac{R}{H}$ = 133.3	T	11.3	43.8	93.8	158.3
	E	11.8	44.3	94.0	154.5
	D	+ 4.4	+ 1.1	+ 0.2	- 2.4
$\frac{R}{H}$ = 157.8	T	20.3	65.7	134.3	221.2
	E	21.2	67.4	131.5	206.7
	D	+ 5.5	+ 2.6	- 2.1	- 6.6
$\frac{R}{H}$ = 179.4	T	7.4	29.9	64.4	109.1
	E	7.8	30.4	64.4	106.3
	D	+ 5.4	+ 1.7	0	- 2.6

*T Theoretical Frequency, H_z

E Experimental Frequency, H_z

D Percent Difference

TABLE 3.4-1 COMPARISON OF THEORETICAL AND EXPERIMENTAL RESONANT FREQUENCIES

For purposes of discussion, a position with the largest displacement was chosen for each arch at each frequency tested and a summary of those points is shown in Table 3.4-2 for symmetrical excitation and in Table 3.4-3 for unsymmetrical excitation. It is not intended to mean that this position is representative of the remaining positions on the arch, but rather as a position having the most precise experimental value.

For forced frequencies, good agreement between theory and experiment was obtained for all tests except for four frequencies as shown in Fig. 3.3-6 at 53.0 and 80.2 H_z, Fig. 3.3-7 at 51.9 H_z and Fig. 3.3-12 at 43.0 H_z. It is possible to account for a maximum error of 20 percent by considering the precision of the micrometer probes, errors in measuring the arch radii and errors due to variations in forcing frequencies. Since at the forcing frequencies indicated above, the difference in amplitude between theory and experiment was greater than 20 percent, this error is not due to experimental error alone. As noted previously, arch displacements were very sensitive to variations in radius at certain frequencies and these sensitivities were more pronounced for arches with larger α values. This agrees with the results shown in Table 3.4-2 and 3.4-3. The particular arches tested were not perfectly circular, hence it is possible that the four frequencies yielding poor agreement were in the frequency range where the arch sensitivities were the greatest. Agreement, within experimental error, was obtained for the remaining 28 forcing frequencies presented.

Forcing Freq. / Arch Parameters	*	Ω_1	Ω_2	Ω_3	Ω_4
R/H = 121.2 α = 100.2° R = 5.09" H = 0.042	1	20.1	58.1	85.7	100.2
	2	0	0	0	- 67.5
	3	0.140-0.066	0.085-0.040	0.049-0.020	0.055-0.026
	4	0.144-0.067	0.160-0.075	0.156-0.072	0.087-0.044
	5	1.0%	0.8%	6.3%	3.5%
	6	<5%	<5%	12%	<5%
R/H = 133.3 α = 116.5° R = 5.60" H = 0.042"	1	27.7	**53.0	**80.2	143.3
	2	0	81.9	- 61.4	- 40.9
	3	0.130-0.040	0.084-0.040	0.086-0.040	0.025-0.011
	4	0.201-0.064	0.163-0.083	0.101-0.047	0.068-0.031
	5	2.4%	3.2%	0.5%	3.8%
	6	10%	42%	25%	10%
R/H = 157.8 α = 97.2° R = 5.05" H = 0.032"	1	19.8	35.4	52.1	85.0
	2	0	0	0	- 68.1
	3	0.138-0.050	0.099-0.030	0.106-0.040	0.079-0.035
	4	0.145-0.054	0.130-0.039	0.217-0.089	0.120-0.059
	5	1.6%	1.5%	4.7%	5.4%
	6	<5%	<5%	<5%	<5%
R/H = 179.4 α = 119.2° R = 5.74" H = 0.032	1	22.9	**43.0	80.0	122.5
	2	0	- 79.9	59.9	0
	3	0.097-0.025	0.112-0.026	0.083-0.020	0.038-0.014
	4	0.212-0.055	0.145-0.037	0.107-0.026	0.070-0.027
	5	1.0%	5.4%	0.8%	5.1%
	6	20%	60%	8%	17%

* 1 Ω, Forcing Frequency, H_z

2 ϕ, Angular Position of Point Considered, Degrees

3 G, Range of Support Displacement used in Test, Inches

4 U_A, Range of Measured Absolute Radial Displacements for the Point, Inches

5 Maximum Variation of U_A/G From Average

6 Difference Between Theory and Experiment for the Point

** Large Difference Between Theory and Experiment

TABLE 3.4-2 SUMMARY OF RESULTS FOR SYMMETRICAL EXCITATION

Forcing Freq. / Arch Parameters	*	Ω_1	Ω_2	Ω_3	Ω_4
R/H = 121.2 α = 100.2° R = 5.09" H = 0.042"	1	18.7	34.9	66.7	92.0
	2	- 45.0	45.0	0	67.5
	3	0.123-0.050	0.152-0.030	0.101-0.040	0.080-0.034
	4	0.115-0.043	0.148-0.034	0.144-0.055	0.095-0.047
	5	4.8%	11.1%	3.0%	7.7%
	6	10%	<5%	<5%	<5%
R/H = 133.3 α = 116.5° R = 5.60" H = 0.042	1	30.1	**51.9	84.7	109.3
	2	20.5	61.4	40.9	81.9
	3	0.111-0.050	0.105-0.041	0.084-0.040	0.055-0.029
	4	0.109-0.049	0.128-0.055	0.135-0.063	0.063-0.038
	5	0.6%	5.1%	1.2%	8.4%
	6	<5%	18%	9%	<5%
R/H = 157.8 α = 97.2° R = 5.05" H = 0.032	1	28.0	54.6	77.3	123.2
	2	45.4	0	68.1	22.7
	3	0.135-0.060	0.114-0.045	0.098-0.040	0.043-0.025
	4	0.153-0.073	0.132-0.052	0.114-0.054	0.064-0.035
	5	4.0%	1.1%	8.2%	2.8%
	6	10%	12%	<5%	<5%
R/H = 179.4 α = 119.2° R = 5.74" H = 0.032	1	20.0	39.8	70.1	91.9
	2	20.0	59.9	- 39.9	- 39.9
	3	0.122-0.050	0.112-0.050	0.082-0.035	0.079-0.035
	4	0.116-0.050	0.107-0.051	0.144-0.070	0.093-0.039
	5	2.9%	3.7%	5.7%	5.4%
	6	<5%	8%	<5%	15%

*1 Ω, Forcing Frequency, H_z

2 ϕ, Angular Position of Point Considered, Degrees

3 G, Range of Support Displacement Used in Test, Inches

4 U_A, Range of Measured Absolute Radial Displacement for the Point Inches

5 Maximum Variation of U_A/G From Average

6 Difference Between Theory and Experiment for the Point

** Large Difference Between Theory and Experiment

TABLE 3.4-3 SUMMARY OF RESULTS FOR UNSYMMETRICAL EXCITATION

Other arches in the range $121.2 \leq \frac{R}{H} \leq 179.4$ and $97.2^\circ \leq \alpha \leq 119.2^\circ$ were also tested, however the results have not been presented as the agreement between theory and experiment was equally as good as those presented here. It was believed that the four arches chosen for discussion adequately indicated the effects of changing arch parameters (i.e. R/H and α).

3.5 Closure to Chapter III

Experimental verification has been provided for the theory predicting the dynamic response of circular thin elastic arches under inplane flexural deformations. Although only arches with simply supported boundary conditions having $121.2 \leq \frac{R}{H} \leq 179.4$, $97.2^\circ \leq \alpha \leq 119.2^\circ$ and thicknesses of 0.032 and 0.042 inches were tested, the theory should be valid for arches having other arch parameters and boundary conditions. Considerable care would be required in making the test arches for $\alpha > 125^\circ$ if reliable results are to be obtained. To test arches with $\alpha < 90^\circ$ a shaker table with a force output of greater than 225 lbs. would be required.

Generally, better agreement between theory and experiment was obtained for unsymmetrical than for symmetrical excitations. This can possibly be explained by noting that only one arch support is vibrating under unsymmetrical excitations which in turn perturbs any sensitivities present in the arch one-half the amount that they would be perturbed under symmetrical excitations.

By comparing results for arches with various α and R/H values,

it can be concluded that the degree of agreement between theory and experiment is governed predominantly by the value of α and to a much lesser extent by the value of R/H.

It was calculated theoretically and shown experimentally that under symmetrical excitations, it is impossible to excite unsymmetrical modes. However, under unsymmetrical excitations it is possible to excite symmetrical modes. This can be explained by noting that unsymmetrical displacements are obtained by superimposing a symmetrical displacement plus a rotation.

Although out-of-plane modes were not studied, they were noted to occur at frequencies having values approximately 16 times the frequency of the first flexural mode. This agrees with the observations of Volterra and Morell (15).

Chapter IV

Closure

4.1 Summary

This investigation was concerned with the development of a theory which could be used to investigate the dynamic response of a thin elastic arch subjected to cyclic support movement. Only flexural deflections in the plane of the initial curvature of the arch were investigated. The arch was assumed to be circular having a constant mass and cross-section and the center line was assumed to be inextensible. A closed form solution was obtained for the homogeneous part of the differential equation. The steady state solution was assumed as a series in terms of the free modes of vibration. Since the natural frequencies were spaced sufficiently far apart, it was found that an eight-term series gave accurate results up to three significant figures for arches excited near the fourth mode. Better accuracy was obtained for excitations below the fourth mode. The theory presented is applicable to arches having a number of different boundary conditions such as pinned-end, fixed-end, free-end or any combination of these.

Experimental evaluation of the theory was presented on the basis of pinned-end boundary conditions. Results were presented for four arches having values of $121.2 \leq R/H \leq 179.4$ and $97.2 \leq \alpha \leq 119.2$

degrees. Two thicknesses of 0.032 and 0.042 inches and a width of one inch were used. Other arches were tested in the above range of R/H and α obtaining equally good results, however, the results were not included in this report as the four arches presented cover the range of R/H and α tested sufficiently.

During the experimental stage of the investigation, it was discovered that arches had to be circular within one-half their thickness before reliable test results were obtained. For arches not perfectly circular, the experimental amplitudes were much greater than the theoretical, indicating that some parameter was highly sensitive in arches having a large variation in radius. As a result, the arches did not respond according to theory where the assumption of circular arches was used. Due to the capacity of the shaker table, arches with $\alpha < 90$ degrees were too stiff and could not be tested. It was found that arches with $\alpha > 125$ degrees were too susceptible to any perturbations and were not tested for this range either. On the basis of the series of tests conducted, it was noted that the value of one-half the opening angle predominantly governed the degree of agreement between theory and experiment. The agreement was governed to a much lesser extent by the value of the radius to thickness ratio. On some arches tested, the first out-of-plane mode was noted to occur at a frequency approximately sixteen times the frequency of the first flexural mode which agrees with the observations made by Volterra and Morell (15).

4.2 Problems for Further Study

As a result of this investigation, other problems requiring further study are:

1. Determine what effects concentrated masses attached to the arch have on the magnification ratio.

2. Extend the present theory to include other arch shapes such as a parabola, cycloid, or a catenary.

3. Investigate the dynamic response of arches for large radial displacements i.e. $R \pm u \neq R$.

4. Perform experiments to test the inextensional theory.

5. Investigate the out-of-plane vibrations caused by parametric excitations (i.e. when plane of initial curvature of the arch and the plane of the support displacements do not coincide, parametric excitation will occur).

6. Investigate further, what effect variations in the radius has on the magnification ratio.

References

1. Lamb, H., "On the Flexure and the Vibrations of a Curved Bar", Lond. Math. Soc. Proc., Ser. 1, V. 19, pp. 365-376 (1887-1888).
2. Den Hartog, J.P., "The Lowest Natural Frequency of Circular Arcs", Phil. Mag. Ser. 7, V. 5, No. 28, pp. 400-408 (1928).
3. Love, A.E.H., "A Treatise on the Mathematical Theory of Elasticity", Dover Publications, 4th edition, Chapt. XXI, (1944).
4. Hoppe, R., "Vibrationen eines Ringes in seiner Ebene", J. reine angew. Math., Bd. 73, pp. 158-170 (1871).
5. Bolotin, V.V., "Parametrically Excited Vibrations of Elastic Arches", Dokl. Akad. Nauk. SSSR, V. 83, pp. 537-539 (1952).
6. Bolotin, V.V., "Parametric Excitation of Axisymmetric Vibrations of Elastic Arches", Inzh. Sb. 15, pp. 83-88 (1953).
7. Morley, L.S.D., "The Flexural Vibrations of a Cut Thin Ring", Quart. Journ. Mech. and Appl. Math., V. XI, pt. 4, pp. 491-497 (1958).
8. Archer, R.R., "Small Vibrations of Thin Incomplete Circular Rings", Int. J. Mech. Sci., V. 1, pp. 45-56 (1960).
9. Mindlin, R.L. and Goodman, L.E., "Beam Vibrations with Time-Dependent Boundary Conditions", J. Appl. Mech., V. 17, pp. 377-380 (1950).

10. Eppink, R.T. and Veletsos, A.S., "Analysis and Design of Domes, Arches and Shells, V. II: Analysis of Circular Arches", AFSWC - TR - 59 - 9, Air Force Special Weapons Centre, Kirkland Air Force Base, New Mexico (1959).

11. Eppink, R.T. and Veletsos, A.S., "Dynamic Analysis of Circular Elastic Arches", 2nd Conference on Electronic Computations, ASCE, pp. 477-502 (1960).

12. Eppink, R.T. and Veletsos, A.S., "Response of Arches Under Dynamic Loads", AFSWC - TR - 60 - 53, Air Force Special Weapons Centre, Kirkland Air Force Base, New Mexico (1960).

13. Volterra, E. and Morell, J.D., "A Note on the Lowest Natural Frequency of Elastic Arcs", J. Appl. Mech., V. 27, Trans., ASME, V. 82, Ser. E, pp. 744-746 (1960).

14. Volterra, E. and Morell, J.D., "Lowest Natural Frequency of Elastic Arc for Vibrations Outside the Plane of Initial Curvature", J. Appl. Mech., V. 28, Trans. ASME, V. 83, Ser. E, pp. 624-627 (1961).

15. Volterra, E. and Morell, J.D., "Lowest Natural Frequencies of Elastic Hinged Arcs", J. Acoust. Soc. Amer., V. 33, No. 12, pp. 1787-1790 (1961).

16. Lang, T.E. and Reed, R.E., "A Method for Determining Modal Characteristics of Nonuniform Thin Circular Rings", Tech. Rpt. No. 32 - 252, Jet Propulsion Laboratory, Caltech, Pasadena, California, (1962).

17. Nelson, F.C., "In-Plane Vibration of a Simply Supported Circular Ring Segment", Int. J. Mech. Sci. V. 4, pp. 517-527 (1962).

18. Lang, T.E., "Vibrations of Thin Circular Rings, Part I. Solution for Modal Characteristics and Forced Excitation", Tech. Rpt. No. 32 - 261, Jet Propulsion Laboratory, Caltech, Pasadena, California (1962).

19. Lang, T.E., "Vibration of Thin Circular Rings, Part II. Modal Functions and Eigenvalues of Constrained Semicircular Rings". Tech. Rpt. No. 32 - 261, Jet Propulsion Laboratory, Caltech, Pasadena, California (1963).

20. Takahashi, Shin, "Vibration of a Circular Arc Bar in its Plane", Bulletin of J.S.M.E., V. 6, No. 24, pp. 666-673 (1963).

21. Nelson, F.C., "Frequency Cross-Over of Simply-Supported Circular Ring Segments", J. Frankl. Inst., V. 278, No. 1, pp. 20-27 (1964).

22. Antman, S. and Warner, W.H., "Dynamic Stability of Circular Rods", J. Soc. Indust. Appl. Math., V. 13, No. 4, pp. 1007-1018 (1965).

23. Sokolnikoff, I.S. and Sokolnikoff, E.S., "Higher Mathematics for Engineers and Physicists", McGraw-Hill, 2nd edition, p. 86, (1941).

24. Rae, J.G., "Vibration of Tapered Cantilever Beams", Unpublished M.Sc. Thesis, Dept. of Mech. Eng., University of Alberta (1967).

25. Bolotin, V.V., "Dynamic Stability of Elastic Systems", Holden-Day Series in Mathematical Physics, Chapt. 18, (1964). (Translation of a Russian text written by Bolotin in 1956).

26. Volterra, E. and Morell, J.D., Errata to reference 14, J. Appl. Mech., V. 34, p. 1046 (1967).

27. Popescu, N.D., "Dynamic Stability of Arches, Curved Plates, Rings, and Pipes Submitted to Periodically Variable Stresses", Struct. Eng., V. 48, No. 12, pp. 467-474 (1970).